Petroleum Science 23 (2026) 2309–2329

Contents lists available at ScienceDirect

Petroleum Science

journal homepage: www.keaipublishing.com/en/journals/petroleum-science

Original Paper

Oil-gas conditions of the Proterozoic metamorphic basement reservoirs in the Wensu Salient, Tarim Basin, China

Yuan-Yin Zhang [a,b,c,*], Ze-Zhang Song [d,**], Zhong-Kai Bai [c], Xing-Zheng Liu [e], Zi-Yu Zhang [d]

[a] Institute of Energy, Peking University, Beijing, 100871, China
[b] Inner Mongolia Golden Hydrogen Geological Exploration Co., Ltd., Ordos, 017000, Inner Mongolia, China
[c] Oil and Gas Survey, China Geological Survey, Beijing, 100083, China
[d] China University of Petroleum (Beijing), Beijing, 102249, China
[e] China University of Petroleum (East China), Qingdao, 266000, Shandong, China

ARTICLE INFO

Article history:
Received 16 December 2024
Received in revised form
12 August 2025
Accepted 6 November 2025
Available online 12 November 2025

Edited by Xi Zhang and Jie Hao

Keywords:
Proterozoic Aksu Group
Weathering metamorphic crust
Stratigraphic trap
Late hydrocarbon accumulation
Wensu Salient
Tarim Basin

ABSTRACT

In 2017, Well XWD1 drilled in the Wensu Salient, northwest Tarim Basin achieved the first hydrocarbon discovery in Proterozoic metamorphic rocks within the western basin of China. However, uncertainties regarding reservoir characteristics, hydrocarbon origins, and accumulation mechanisms have constrained further evaluation and exploration planning. Based on various hydrocarbon exploration data and experimental analyses from the region, this study conducts a comprehensive analysis of regional tectonic evolution, reservoir characterization, and hydrocarbon source correlation. Furthermore, it establishes a hydrocarbon accumulation model for metamorphic rock reservoirs and assesses their resource potential. It is found that: 1) the metamorphic strata have suffered extensive uplifts and denudations since the Paleozoic till the late Neogene, and extensively reformed by a northeast-trending boundary fault system, thus resulting fractured weathering crust reservoirs beneath the regional unconformity; 2) the metamorphic reservoirs exhibit ultra-low porosities typically around 4%, and low permeabilities ranging from 0.061 mD to 1.5 mD; 3) the discovered crude oil is characterized of typical terrestrial genesis associated with the northeastern Baicheng Sag, and was accumulated at approximately 17 Ma and 5 Ma; 4) the collected gas featured a mixed origin, which might derive from overmature marine source rocks in the Awati Sag, the marine oil cracking, and terrestrial source rocks in the northeastern Baicheng Sag, respectively; 5) the most promising metamorphic traps cover an area of 386.7 km^2, with a preliminary resource estimate of up to 57 million tons, implying significant exploration potential.

1. Introduction

Basement rocks possess the potential to form significant reservoirs globally and offer promising hydrocarbon explorations. Among the hundreds of industrial-level basement oil and gas fields discovered worldwide, metamorphic oilfields account for 40% of the total (Areshev et al., 1992; Koning, 2003; Ma et al., 2006; Parnell et al., 2017; Xu et al., 2024), such as the Precambrian Nafoora oilfield in the Sirte Basin, Libya (Burwood et al., 2003; Tian et al., 2008), the Rona Ridge Lancaster, Edvard Grieg and Johan Sverdrup fields on the UK and Norwegian continental shelfs in the North Sea (Riber et al., 2015; Trice et al., 2022), and the metamorphic oilfield in the Bongor Basin, Chad (Ma et al., 2006; Yu et al., 2019; Dou et al., 2020). These reservoirs are primarily developed in the weathering crust at the buried-hills or paleo-highs and are sometimes found within the basement (Schubert et al., 2007; Gao et al., 2008; Meng et al., 2009; Jin et al., 2014; Liu et al., 2020). Basement reservoirs typically undergo multiple stages of tectonic activity and diagenetic processes and are predominantly characterized by secondary pores and fractures, exhibiting substantial heterogeneity and anisotropy (Krishna, 2003; Wang et al., 2015, 2019; Belaidi et al., 2018; Bonter and Trice, 2019; Liu et al., 2020; Zhang et al., 2023). They are usually adjacent to or in communication with neighboring fertile source rocks through an

* Corresponding author.
** Corresponding author.
E-mail addresses: zhangyuanyin@pku.edu.cn (Y.-Y. Zhang), songzz@cup.edu.cn (Z.-Z. Song).

Peer review under the responsibility of China University of Petroleum (Beijing).

https://doi.org/10.1016/j.petsci.2025.11.016

efficient drainage system and regionally sealed by overlying cap rocks (Meng et al., 2009; Yu et al., 2019; Xue et al., 2021).

Since the discovery of the Yaerxia Oilfield in the Jiuquan Basin in 1956, China has identified several basement oilfields with considerable reserves. These basement reservoirs vary in geological age across different regions: in the eastern basins of China, they are primarily Archean formations (e.g., Bohai Bay Basin and Hailar Basin); in the offshore basins of southeastern China, they mainly consist of Mesozoic strata (e.g., East China Sea Basin, Pearl River Mouth Basin, and Qiongdongnan Basin); whereas in the central and western basins, they are predominantly Paleozoic formations (e.g., Tarim Basin and Jiuquan Basin) (Meng et al., 2009; Tong et al., 2012; Liu et al., 2020; Ye et al., 2022; Lyu et al., 2023). Overall, the discovered basement hydrocarbon reservoirs in China are predominantly oil-bearing, with relatively few gas reservoirs. The reservoir lithologies mainly consist of granite, volcanic rock, clastic rock, and carbonate rock. Petroleum exploration in metamorphic basement reservoirs is primarily distributed in the Bohai Bay Basin in eastern China, while the petroleum potential and conditions of basement reservoirs in western sedimentary basins have been overlooked (Lyu et al., 2023).

The Wensu Salient is located at the northwestern margin of the Tarim Basin in western China and represents a persistent paleo-uplift. Its basement consists of Proterozoic Aksu Group strata, overlain primarily by Cenozoic deposits with minor occurrences of Neoproterozoic to Early Paleozoic formations. The lithology of the Aksu Group is predominantly composed of blueschist-greenschist facies rocks, with mineralogical studies indicating that the blueschists underwent metamorphism at temperatures of 300–400 °C and pressures of 4–6 kbar (Liu et al., 2017).

Based on petrographic and geochemical analyses, previous studies have reconstructed the protoliths of the Aksu Group metamorphic rocks as sandstone and greywacke, suggesting that they were deposited in a sedimentary basin near a continental island arc. The sediments were likely derived from the weathering and erosion of felsic volcanic rocks associated with island arc tectonic activity (Qi et al., 2011; Liu et al., 2017, 2021). Furthermore, extensive geochronological investigations using Rb–Sr, $^{40}Ar/^{39}Ar$, and U–Pb dating methods have constrained the metamorphic age of the Aksu Group to 760–820 Ma (Long et al., 2010; Dong et al., 2011; Chang et al., 2012; Zhang et al., 2013, 2014; Ge et al., 2014; He et al., 2014; Ding et al., 2015; Liu et al., 2017; Chen et al., 2020), corresponding approximately to the breakup of the Rodinia supercontinent. Subsequently, the Wensu Salient has experienced complex tectonic activity. Field outcrop observations and seismic data analyses have confirmed that it is an inherited structure controlled by boundary faulting and basement uplift (Qi et al., 2011; Liu et al., 2017, 2022).

The Wensu Salient has undergone prolonged uplift and erosion, and it does not host source rocks. Consequently, the metamorphic rock strata of the Aksu Group have not previously been considered as potential hydrocarbon reservoirs, and related research has been lacking (Zhang et al., 2019). In 2017, the XWD1 well encountered hydrocarbons in the weathered crust layer of the Aksu Group basement, followed by three additional wells achieving hydrocarbon breakthroughs in the same interval. This marked the first discovery of hydrocarbons in China's western basins within an extremely ancient stratigraphic unit (the Proterozoic metamorphic section of the Aksu Group) and at shallow depths (burial depths ranging only from 997.4 to 1017 m). However, the reservoir characteristics and hydrocarbon origins of these metamorphic rocks remain unclear. The accumulation characteristics, distribution patterns, and resource potential of the hydrocarbons are also poorly understood, posing significant challenges to evaluation and deployment.

Although effective source rocks are not developed within the Wensu Salient itself, various types of source rocks with different hydrocarbon generation and expulsion timings are developed in the surrounding depressions. Clearly, the key scientific issues in constructing a hydrocarbon accumulation model for the Aksu Group metamorphic reservoirs lie in determining the timing of trap formation under complex tectonic activities, identifying the sources and charging time of hydrocarbons, and clarifying the migration pathways.

Accordingly, based on various hydrocarbon exploration data from the Wensu Salient, this study first analyzes the tectonic evolution history since the formation of the basement, as well as the present characteristics and distribution patterns of the weathered crust reservoirs. Subsequently, a comprehensive review of the hydrocarbon source rock conditions in the surrounding areas of the Wensu Salient is conducted, and geochemical analyses of crude oil and natural gas samples are performed to determine the sources of oil and gas within the metamorphic reservoirs. Finally, by examining hydrocarbon migration pathways and accumulation periods, this study, for the first time, constructs a hydrocarbon accumulation model for the metamorphic reservoirs of the Aksu Group in the Wensu Salient and provides a preliminary assessment of resource potential. The findings aim to support subsequent exploration planning and offer valuable insights for similar geological settings.

2. Geological setting

The Wensu Salient is strategically situated at the intersection of multiple tectonic units within the Tarim Basin, representing a long-lived residual paleo-uplift. It is classified as a critical tectonic feature within the northwestern segment of the basin, essentially belonging to a prototypical basin-mountain transition zone (Jia et al., 1995; Jia, 1997; He et al., 2011; Zhang et al., 2019; Paridiguli et al., 2020; Liu et al., 2022). Oriented in a northeast-southwest direction, the Wensu Salient encompasses an extensive area of approximately 4500 km^2 and is peripherally delineated by four significant fault systems: the primary Karayuergun fault to the north, the primary Gumubez fault to the west, the primary Shajingzi fault to the east, and the secondary Yingan fault to the south, respectively (Fig. 1(b)). It is encircled by three sedimentary sags on the plane, namely the Baicheng sag in the northeast, the Awati sag in the southeast, and the Wushi sag in the northwest, respectively (Fig. 1(b)).

The stratigraphy of the Wensu Salient, as observed in Well WC1 (Fig. 1(c)), exhibits a vertical succession ranging from the Cenozoic Quaternary (Q), Neogene (N), Sinian (Z) to the Proterozoic Aksu Group (Pt_2ak) from top to bottom. Pt_2ak serves as the regional basement, characterized by a pronounced angular unconformity with overlying Sinian and Neogene strata (Fig. 2), indicating its ancient uplift status. It trends northeastward and presents a gradual uplift from the northeast towards the southwest (Fig. 2 BB_1), as evidenced by field exposures, drilling cores, and seismic data (Zhang et al., 2019, 2022a; Liu et al., 2022).

The Aksu Group primarily comprises thick layers of grey–green chlorite schist and blue quartz schist, a product of regional low-temperature, high-pressure metamorphism and magmatic activities during the Proterozoic era (Qi et al., 2011; Liu et al., 2017, 2021; Wu et al., 2022). The limy dolomite, dolomitic mudstone, and mudstone deposits generally mark the overlying Sinian strata.

The Wensu Salient represents an inherited residual ancient uplift with a protracted development history spanning from the Middle–Late Ordovician to the Neogene period (Jia et al., 1995; Jia, 1997; He et al., 2011; Zhang et al., 2019; Liu et al., 2022). During the Neogene, extensive subsidence led to the accumulation of

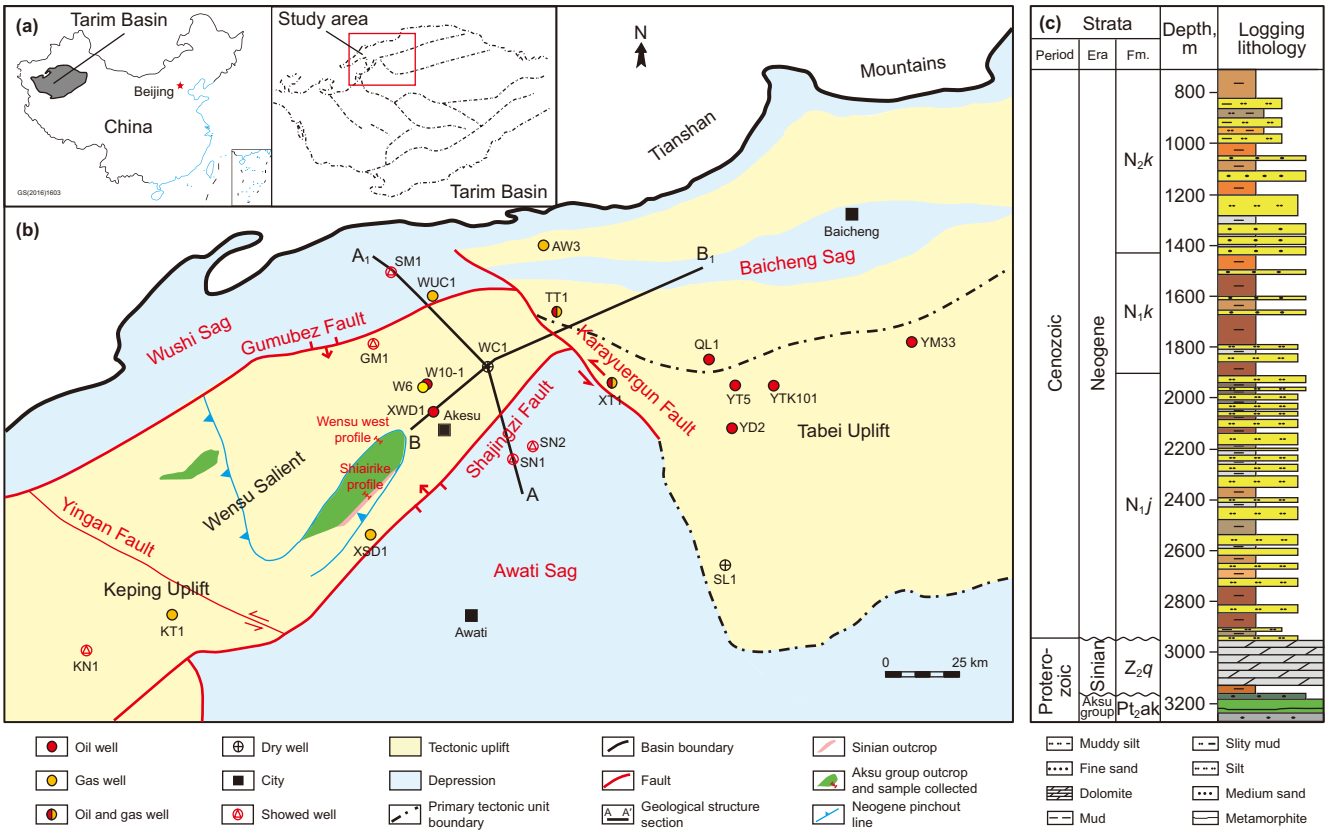

Fig. 1. **(a)** Location of the research area within the Tarim Basin, China. **(b)** Tectonic units in the Wensu Salient, indicating the locations of typical wells and research sections. **(c)** The lithology of the formations identified by the logging of Well WC1.

abundant terrigenous debris from the northern Tianshan Mountains (Zhang et al., 2019; Liu et al., 2022). Consequently, the Neogene sequence in this region primarily comprises clastic deposits, which are further subdivided into the Kuqa Formation (N_2k), Kangcun Formation (N_1k), and Jidike Formation (N_1j), respectively (Fig. 1(c)). In addition, the possibility of lower Paleozoic strata exists in the flanks of the Wensu Salient, and the Precambrian strata are commonly exposed in the southwestern part of the study area (Fig. 2 BB_1).

Early hydrocarbon exploration in the Wensu Salient suggested the absence of hydrocarbon source rocks, coupled with a thin Cenozoic cap and underdeveloped effective traps, which led to the region not being prioritized for hydrocarbon exploration. However, since 2017, high-yield oil flows have been continuously discovered within the clastic strata of the Cenozoic Jidike Formation, and by 2024, the region had developed into a high-quality oil field with an annual output of 600,000 tons of oil equivalent, demonstrating its vast exploration and development potential. The Jidike Formation features large-scale deltaic beach-bar sand bodies with excellent reservoir properties, including an average porosity exceeding 20% and average permeability greater than 100 mD, forming various types of traps with the overlying mudstone. Source rock analysis confirms that the oil and gas in the Cenozoic sandstone reservoirs of the Wensu Salient primarily originated from the terrigenous hydrocarbon source rocks in the Baicheng Sag to the northeast, with overall late-stage accumulation (Zhang et al., 2019, 2022a, 2022c).

In addition, hydrocarbons have been encountered in the Silurian formation of Well XSD1 in the Shajingzi structural belt on the southeastern margin of the Wensu Salient and in the Permian formation of Well SN1 in the Shanan structural belt in the northwestern Awati Sag. Source rock correlation analysis indicates that these hydrocarbons originate from marine source rocks in the Awati Sag (Zhang et al., 2022b, 2022d).

By contrast, the discovery of oil patches and traces within the bedrock weathering crust interval (997.4–1017 m) of the Proterozoic Aksu Group by Well XWD1 in 2017 marked a significant milestone. The gas logging data from this well indicated a whole-hydrocarbon peak value of 2.88%, and logging interpretation suggested the presence of a 14.3 m fractured reservoir in the bedrock (Fig. 3). Subsequent pumping tests in the open hole section (939.44–1058 m) of Well XWD1 using a 73 mm oil tube yielded a total oil production of 2.19 m^3. Encouraged by this initial success, six additional wells were drilled through the weathering metamorphic reservoirs in the area, with three of them (Wells W6, W6-1, and W10-1) undergoing oil and gas testing that resulted in commercial productions. Specifically, Wells W6 and W6-1 produced daily gas volumes of 2.85 × 10^4 m^3 and 2.34 × 10^4 m^3, respectively, while Well W10-1 produced 2.6 m^3 of oil per day during casing testing.

This metamorphic basement reservoir is generally shallow in burial depth and exhibits diverse types of hydrocarbon accumulations, with the lower mudstone of the Neogene serving as an effective regional seal. However, uncertainties remain regarding its reservoir characteristics and hydrocarbon sources, as well as the accumulation characteristics, distribution patterns, and resource potential. These knowledge gaps have constrained further evaluation and exploration planning in the region.

Given a thick mudstone caprock at the base of the Jidike Formation, the bedrock weathering crust within the Aksu Group is increasingly viewed as another promising hydrocarbon exploration target in the Wensu Salient. However, further exploration and

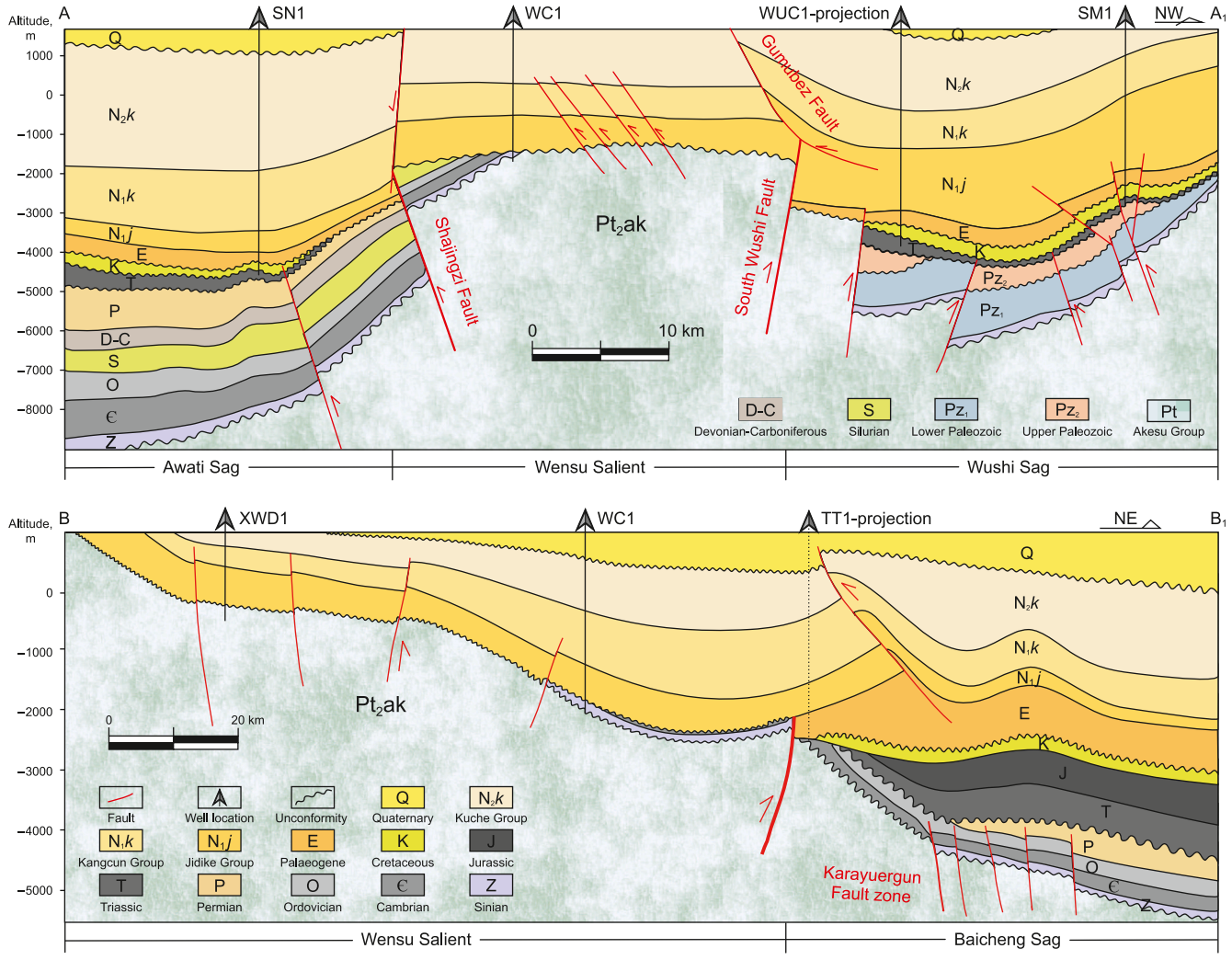

Fig. 2. Geological profile map of the study area (section locations are AA_1 and BB_1 in Fig. 1).

exploitation efforts inevitably necessitate comprehensive research into the oil and gas conditions, the accumulation model and potential. Understanding the geological processes that led to the formation of these reservoirs and the distribution and quality of the hydrocarbon resources they contain will be crucial in guiding future exploration activities in the region.

3. Materials and Methodology

To analyze the characteristics of the metamorphic weathered crust reservoir, seventeen reservoir samples from representative drillings and outcrop examinations in the Aksu Group were meticulously selected for thin-section analysis. These samples were prepared using vacuum impregnation with blue epoxy resin to accentuate the pore spaces. The thin-section observations facilitated the identification of intergranular pore-filling minerals and the classification of pore types. Subsequently, the samples were reduced to ultrafine particles with a diameter of less than 40 μm. X-ray diffraction (XRD) analysis was conducted to ascertain the mineralogy by utilizing a typical focus Cobalt X-ray tube in a Siemens Diffractometer D8 operated at 40 mA and 40 kV. Porosity and permeability measurements were systematically undertaken by inserting sample plugs into a permeameter and injecting nitrogen at 100 psi and 400 psi confining pressures.

To conduct a hydrocarbon correlation analysis of the metamorphic reservoir, twelve crude oil samples were gathered to analyze the whole-oil gas chromatography gas chromatography-mass spectrometry (GC–MS) of the saturated hydrocarbons and aromatics. Whole-oil gas chromatography was carried out using an Agilent 6890 N gas chromatograph (Li et al., 2010a). The chromatographic column was maintained at 40 °C for 7.5 min, followed by heating from 40 °C to 90 °C at a rate of 15 °C per minute and then from 90 °C to 180 °C at 6 °C per minute. Helium served as the carrier gas throughout this process. An Agilent 6890–5975 GC–MS system was employed to analyze saturated hydrocarbons and aromatics quantitatively. The temperature program for saturated hydrocarbon chromatography started at 50 °C for 2 min, then increased to 100 °C at a rate of 2 °C per minute, and finally rose to 310 °C at 3 °C per minute for 30 min. Subsequently, the temperature program for aromatic hydrocarbon chromatography was set to start at 60 °C, increase to 150 °C at 8 °C per minute, and then to 320 °C at 4 °C per minute, where it was held constant for 10 min. Helium was used as the carrier gas for both analyses, and the data were processed and analyzed using an Agilent Chemstation.

Thirty-three gas samples from the Neogene, Aksu Group, and Cambrian reservoirs in the central area of and surrounding the Wensu Salient were collected for natural gas composition analysis. In addition, 12 carbon isotope analyses were conducted. The

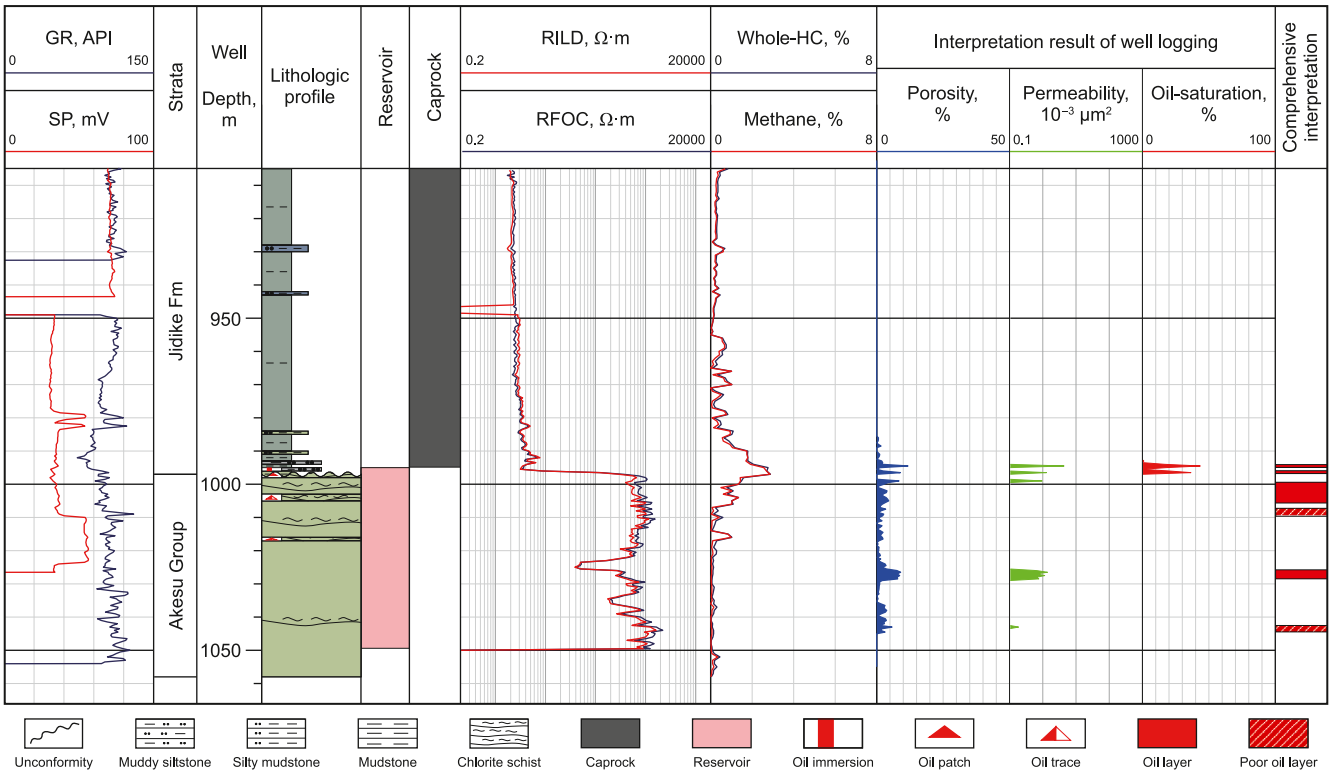

Fig. 3. Comprehensive histogram of four properties of weathering metamorphic intervals in Well XWD1.

natural gas composition experiments were carried out using an Agilent 6890 N gas chromatograph (G.C.) as the natural gas analyzer, following the detection standards of GB/T 13610-2020 and GB/T 11062-2020 to determine the gas composition of natural gas samples. The carbon isotope analysis of natural gas was conducted using an Optima isotope ratio mass spectrometer and a Hewlett-Packard 6890 II gas chromatograph to determine gas samples' stable carbon isotope values. The analysis adhered to the detection standard of SY/T 5238-2008. The hydrocarbon gas components were separated by gas chromatography and converted to CO_2 at the combustion interface before being introduced into the mass spectrometer (M.S.). A fused silica capillary column (30 mm × 0.32 mm) was used, with the oven temperature initially at 35 °C, increasing at a rate of 8 °C/min to 80 °C, and then at a rate of 0.5 °C/min until it reached 260 °C, where it was held for 10 min. The gas isotope ratios are expressed as "δ" with units of "‰". The measurement precision for $\delta^{13}C$ is ±0.1‰.

All experiments and analyses related to reservoir and oil-gas samples described in this paper were conducted at the State Key Laboratory of Petroleum Resources and Engineering, China University of Petroleum (Beijing). Additionally, this study conducts a structural evolution analysis based on NW-trending cross-sections traversing the Wensu Salient and its surrounding sags, highlighting the prolonged erosion, leaching history, and potential trap characteristics of the metamorphic weathered crust reservoir. Furthermore, by systematically reviewing previous studies on source rocks in the Baicheng Sag and Awati Sag, this study evaluates the hydrocarbon potential of the Wensu Salient.

4. Results

4.1. Tectonic evolution and weathering history

The North Tarim craton was substantially amalgamated from several blocks during convergence associated with the assembly of the Rodinia supercontinent, whereas the South Tarim Craton was adjacent to north Australia (Long et al., 2010; Dong et al., 2011; Ge et al., 2014; He et al., 2014; Zhang et al., 2014; Ding et al., 2015; Wu et al., 2018, 2021). Subsequently, it became an active continental margin and gradually formed a regional orogen due to the extensive southward subduction of the pan-Rodinia oceanic crust. This orogenic complex comprised Paleoproterozoic metamorphic successions and Proterozoic rifted magmatic rocks. The Aksu Group, predominantly composed of blueschist and greenschist, thus serves as the metamorphic basement in the northwest Tarim Basin (Zhang et al., 2009; Qi et al., 2011; Zhu et al., 2011; Liu et al., 2017, 2021) with depositional ages preceding approximately 820 Ma and metamorphic ages preceding approximately 760 Ma, as evidenced by the ages of 757 and 759 Ma for mafic dikes (Zhang et al., 2009, 2014). The North Tarim orogeny underwent complex extension and significant denudation during the breakup of the Rodinia supercontinent at approximately 740–600 Ma, which was broadly terminated by a widespread transgression accompanied by late Ediacaran and Early Cambrian depositional events (Wu et al., 2022).

After that, the Wensu Salient gradually represented a residual paleo-uplift that has undergone prolonged development and is primarily governed by boundary faults (Jia, 2005; Cui and Tang, 2011; Wang et al., 2009; Qi et al., 2014; Paridiguli et al., 2020; Liu et al., 2022; Zhang et al., 2022d). The corresponding evolution can be categorized into five stages, based on the structural evolution analysis through the NW-trending cross-section traversing the Wensu Salient and its surrounding sags (Fig. 4):

(1) **Basement formation stage:** Before the deposition of the Ordovician system, the remaining Sinian and Cambrian sequences in the northwest and southeast of the Wensu Salient exhibited essentially a consistent thickness and similar structures, suggesting the relatively stable sedimentation and undeveloped boundary faults at that time (Fig. 4(a)).

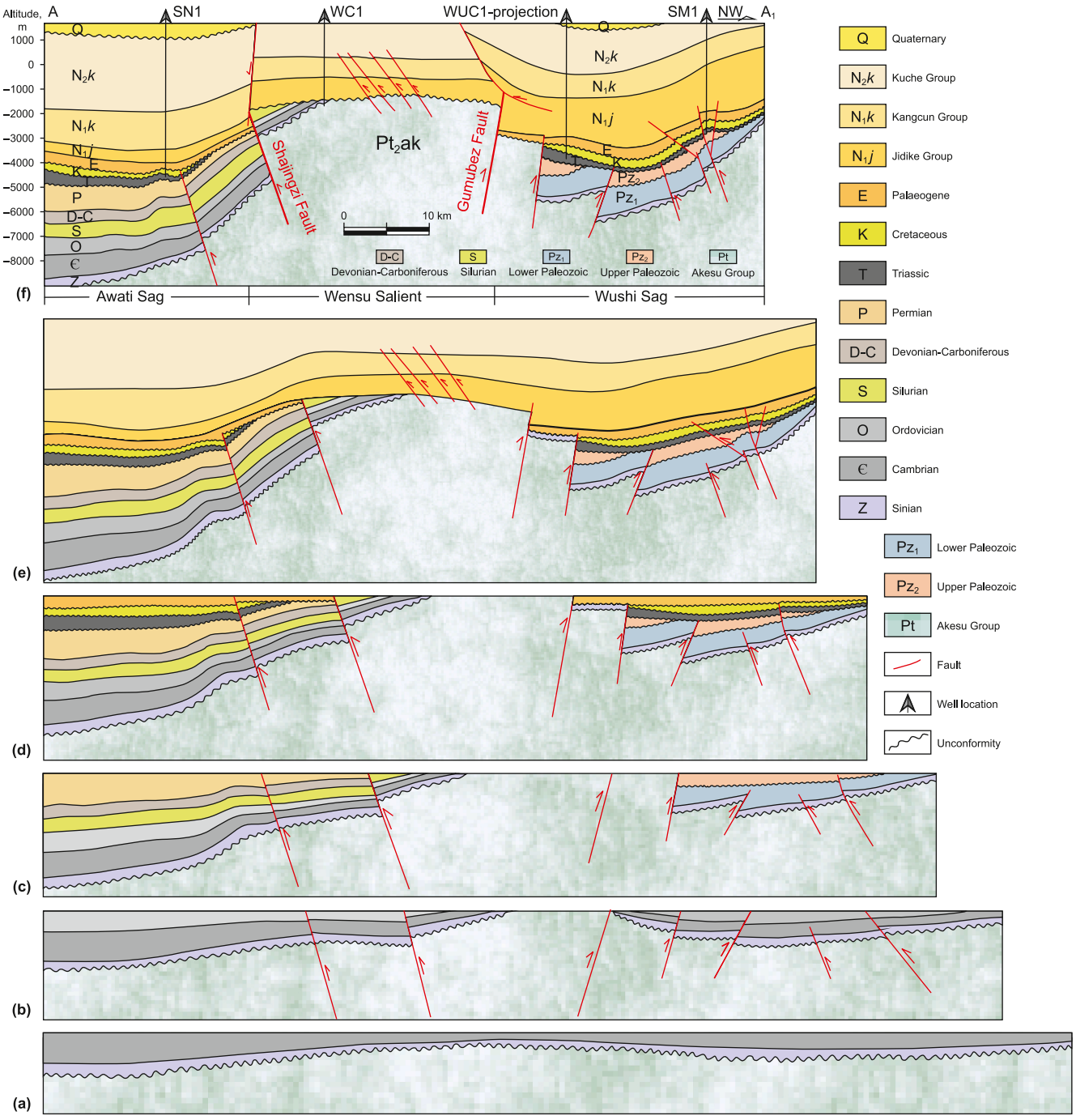

Fig. 4. Tectonic evolution profile across the Wensu Salient and adjacent sags at critical geology periods (The section is mapped in Fig. 1(b)). **(a)** Cambrian–Ordovician transition: tectonic stabilization period. **(b)** Ordovician–Silurian transition: forming the initial paleo-uplift. **(c)** Permian–Triassic transition: suffering severe thrust and erosion. **(d)** Early Miocene: consistent thrust and erosion. **(e)** Early Quaternary: regional subsidence. **(f)** Current section.

(2) **The initiation stage of the ancient salient**: During the Ordovician until the Silurian sedimentary period, the Tarim Basin experienced compression, resulting in a series of southward-thrusting faults and associated folds in the northern region, which controlled the northern boundary of the Wensu Salient. Simultaneously, the Shajingzi deep thrust wedge began to form, governing its southern boundary (Qi et al., 2014; Zhang et al., 2022d). During this stage, the prototype of the Wensu Salient started to take shape, and the higher positions began to undergo erosion (Fig. 4(b)).

(3) **The intense thrusting and erosion stage:** During the Silurian to Devonian period, influenced by the deep thrust wedge of the Shajingzi fault, the Wensu Salient continued to be uplifted, and the strata of the Wushi Sag were also elevated. At the end of the Permian to the Early Triassic, affected by the collisional orogeny of the South Tianshan, the Shajingzi fault underwent intense thrusting towards the

Awati Sag, leading to the extensive strata erosion in the core of the Wensu Salient and forming its basic morphology (Fig. 4(c)).

(4) **The persistent thrusting and erosion stage:** During the Triassic to the Paleogene period, both the Gumubez and Shajingzi faults remained active, and the Wensu Salient continued to be elevated. The Mesozoic strata were absent in the core of the Salient, with only the Cretaceous and Paleogene strata developing on its periphery, forming an unconformity with the underlying strata (Fig. 4(d)). During the continuous uplift of the Wensu Salient, the Paleozoic-Mesozoic strata underwent extensive denudation, leading to the intense weathering and erosion of the Aksu Group's metamorphic rock layers.

(5) **The sedimentary-thrusting-overall subsidence development stage:** Before the deposition of the Jidike Formation (N_1j), the Wensu Salient was affected by the far-field effects of the Himalayan orogeny, leading to the development of a series of secondary faults within the uplift. These faults further modified the conditions of the metamorphic reservoir, and their distribution characteristics will be discussed in detail in the Discussions of this paper. During the middle to late stages of Kuqa Formation (N_2k) deposition, the Wensu Salient ceased its uplift activity and subsequently experienced stable sedimentation, ultimately shaping its present-day structural framework (Fig. 4(e) and (f)).

Therefore, although the metamorphic strata of the Aksu Group in the Wensu Salient are ancient and have lost nearly all primary porosity, prolonged uplift, erosion, weathering, and leaching over hundreds of millions of years, coupled with extensive modification by secondary faults during the Cenozoic, have facilitated the development of high-quality metamorphic weathered crust reservoirs at the top of these formations.

As the basement of the Wensu Salient generally tilts and uplifts toward the southwest, outcrops of the Aksu Group can be observed along its southwestern margin (represented by the green formations in Fig. 1(b)). In the Wensu West section, the exposed greenschist formations of the Aksu Group exhibit well-developed structural fractures and joint networks (Fig. 5(a)), along with a characteristic spheroidal weathering morphology. Differential weathering has resulted in the formation of cavities, with some fractures filled by quartz veins (Fig. 5(b)), indicating the typical weathered crust features of metamorphic rocks.

In the Shiairike section, a clear angular unconformity can be observed between the Proterozoic Aksu Group and the Sinian Sugaitbulak Formation (Fig. 5(c) and (e)–(f)). The strata above the unconformity mainly consist of hard, dense, reddish-purple sandstone (Fig. 5(d)), which has historically been used by local residents as a whetstone. Below the unconformity, the metamorphic rock layers are generally fragmented, exhibiting multiple phases of faulting and fracturing, with some fractures filled with surface-derived yellow and brown clay, indicating a high degree of weathering.

Based on this observation, it can be inferred that in the central-eastern core area of the Wensu Salient, where the Aksu Group is unconformably overlain by Neogene strata, the metamorphic basement surface has undergone a longer weathering duration. This extended weathering process is likely to have enhanced reservoir quality, making it a favorable target for hydrocarbon accumulation.

4.2. Weathering metamorphic reservoir characteristics

The lithofacies of the selected Proterozoic Aksu Group samples are mainly identified as the quartz-fibered mica schist and the chlorite schist. The schist is characterized by its tightness and often exhibits rhythmic deformation structures and layering of distributed minerals. The mineral composition is predominantly composed of quartz, plagioclase, and clay minerals in descending order, with average contents reaching 35.3%, 28.5%, and 23.3%, respectively (Fig. 6). Potassium feldspar is the fourth most abundant mineral, with an average content of 6.1%. Pyrite and anhydrite share the same average content of 6%, constituting the fifth component. Calcite is rarely present and has the lowest content of 0.8%.

Pore morphology indicates that the weathering metamorphic reservoir space in the Wensu Salient is predominantly controlled by tectonic fractures, as evidenced by the frequent occurrence of oil-stained fracture surfaces (Fig. 7(a)). The observed joints are tightly spaced with gaps of less than 0.1 mm, while the tectonic fissures are relatively wider, ranging in width from 0.5 mm to 3 mm. These fissures suggest a tendency to interconnect and are capable of hosting hydrocarbons.

Core photograph observations of the metamorphic rock reservoir section show that the cores are well-preserved, with the fresh surfaces mainly showing a greyish-green color (Fig. 8(b)and(c)). The rock composition is chiefly made up of the chlorite and quartz, displaying a schistose structure and a metamorphic texture. The rocks demonstrate considerable hardness and are generally compact. However, core photographs from Well XWD1 show a high level of fracturing. In the interval ranging from 997.83 m to 998.26 m, 18 minor fractures at various angles were identified. Significantly, four more significant fractures with a 30-degree strike direction were noted, measuring 5–12 cm in length and 1–2 cm in width, all filled with greyish-brown crude oil. The core samples from this area generally display poor reservoir properties, with the porosity ranging from 1.4% to 11.8% and in situ matrix permeability varying from 0.061 mD to 1.5 mD, respectively. In contrast, the interpretation of current logging data statistically indicates an average porosity of 3% and an average permeability of 1 mD (Fig. 3). These values can be essentially categorized as ultra-low porosity (<10%) and low-permeability (0.1–10 mD) (Jiang et al., 2015).

Basement reservoirs are broadly classified into weathered crust reservoirs, located at structural elevations, and interior fault-related basement reservoirs. These reservoirs typically have undergone multiple phases of tectonic activity and diagenesis, leading to the development of natural fractures and secondary pores, making them highly heterogeneous (Bonter and Trice, 2019; Liu et al., 2020; Zhang et al., 2023; Trice et al., 2022). Analysis based on field outcrops and existing well data indicates that the dominant reservoir spaces in the weathered crust of the metamorphic reservoir in the Aksu Group of the Wensu Salient are primarily fractures and dissolution cavities (Fig. 8(b) and (c)). These reservoir spaces are mainly distributed within the upper 50–100 m of the weathered crust and are closely associated with faults formed through multiple phases of tectonic modification, as illustrated in the reservoir development schematic diagram (Fig. 8(a)).

Integrating the structural evolution history discussed in Section 4.1, the evolutionary history of the metamorphic weathered crust reservoir can be reconstructed as follows: Around 820 Ma, the Wensu Salient underwent the deposition of pyroclastic materials, forming the initial Aksu Group strata. With subsequent

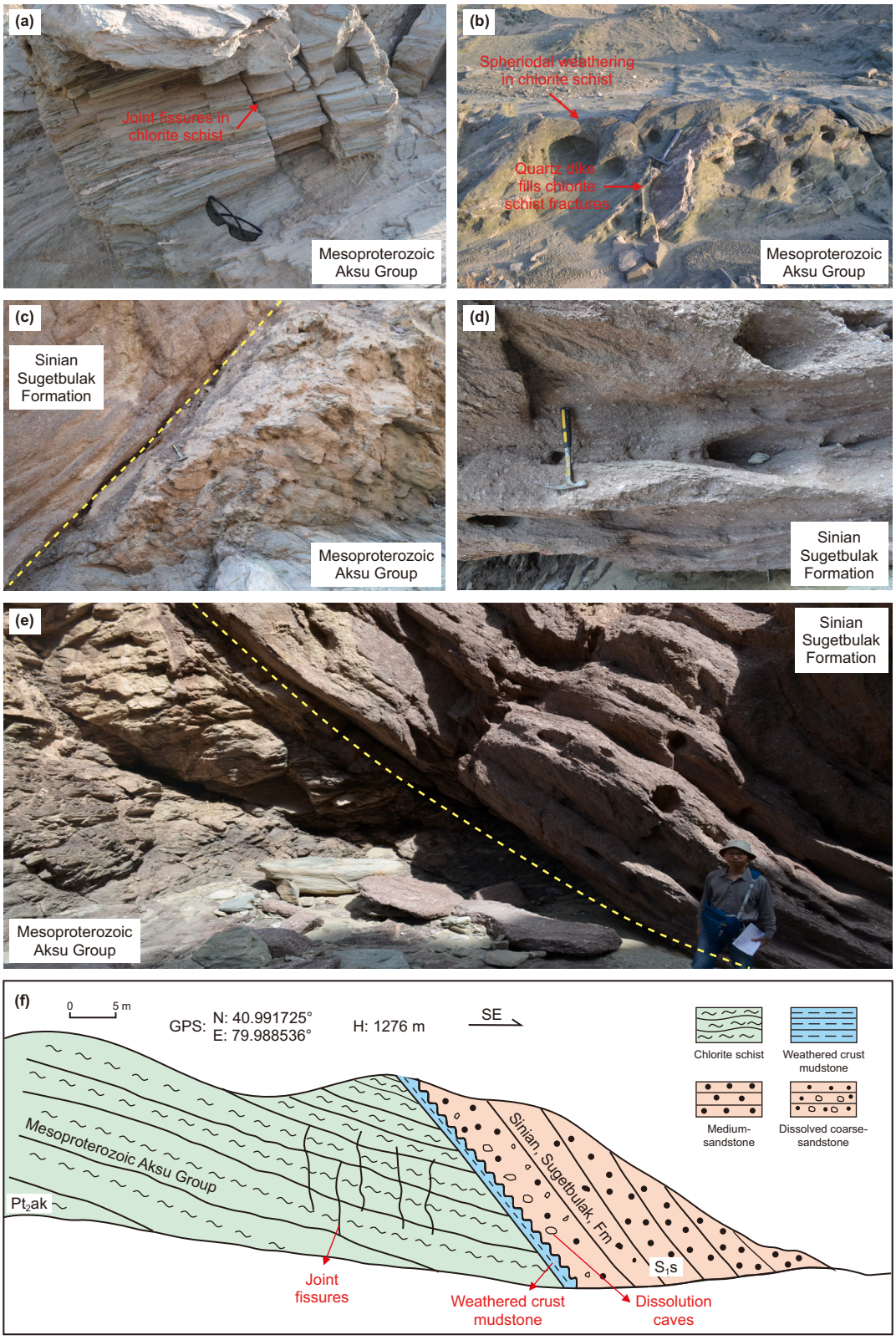

Fig. 5. Typical outcrops and field sketch cross-section of the Aksu Group in the study area. **(a)** Joint fissures in quartz schist in Aksu Group. **(b)** Aeolian spheroidal weathering in Aksu Group. **(c)** Angle disconformity between Aksu Group and Sinian. **(d)** Dissolution pores in Sinian Sugetbulak Formation. **(e)** Angle disconformity between Aksu Group and Sinia. **(f)** Sketch cross-section of the angle disconformity.

compaction and diagenesis, reservoir porosity gradually decreased. Around 760 Ma, the Aksu Group experienced metamorphism, leading to the near-complete disappearance of reservoir spaces (Long et al., 2010; Dong et al., 2011; Chang et al., 2012; Zhang et al., 2013, 2014; Ge et al., 2014; He et al., 2014; Ding et al., 2015; Liu et al., 2017; Chen et al., 2020). This was

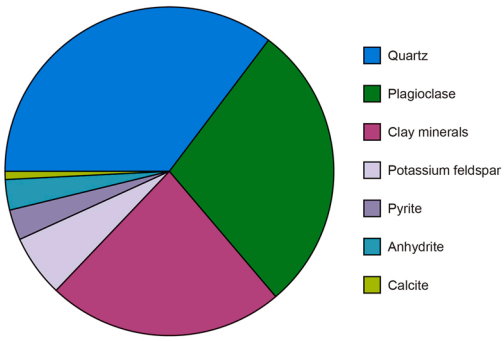

Fig. 6. Mineral composition of the weathering metamorphic reservoirs in the Wensu Salient.

followed by a prolonged period of uplift and erosion, which led to the formation of the weathered crust reservoir at the top of the metamorphic rocks. Around 600 Ma, the uplifted surface was subjected to Sinian–Early Ordovician sedimentation, forming an unconformity.

During the Paleozoic to Early Cenozoic, the Wensu Salient experienced continuous tectonic uplift, thrusting, erosion, and weathering-leaching, which largely removed the Sinian-Palaeogene sediments (Fig. 4(a)–(d)). This process further enhanced the quality of the metamorphic weathered crust reservoir. It was not until the mid-late Neogene that the uplift ceased, allowing stable sedimentation (Fig. 4(e) and (f)). The lower section of the Jidike Formation mudstone (with an average thickness of 80–100 m, Zhang et al., 2019) directly overlaid the metamorphic reservoir, forming an effective seal.

4.3. Source rock conditions

The Wensu Salient is generally devoid of source rocks. However, previous studies have confirmed the presence of source rocks in both the northeastern continental petroleum system within the northeastern Baicheng Sag and the southeastern marine

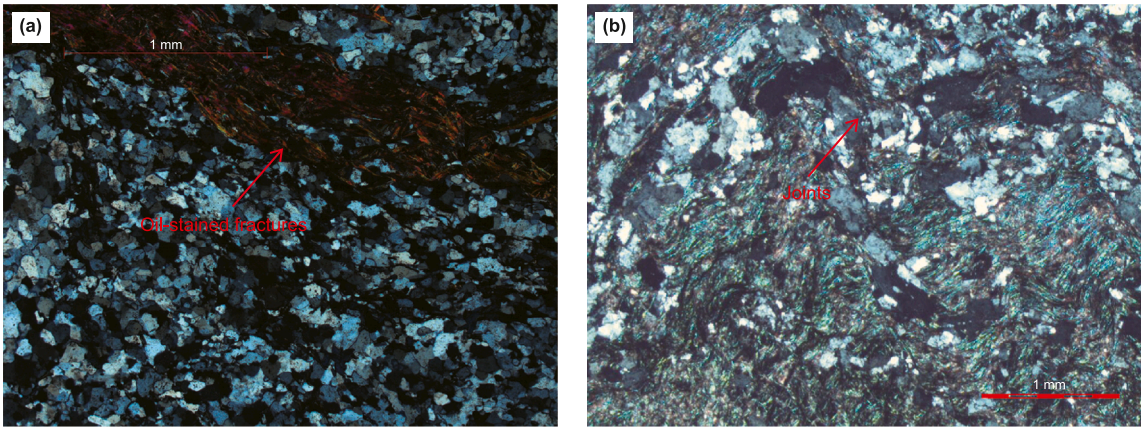

Fig. 7. Pore morphology of the weathering metamorphic reservoir in the Wensu Salient. **(a)** Well XWD1, 998.6 m depth. **(b)** Outcrops in the Tuomuer profile.

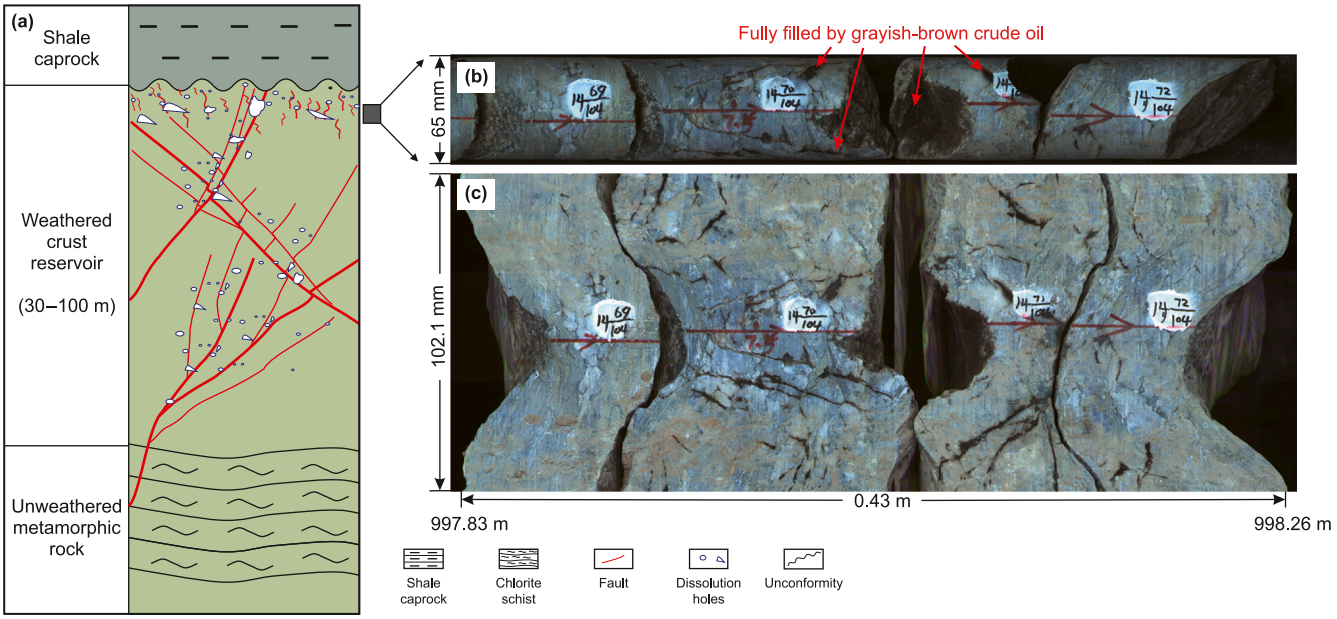

Fig. 8. Aksu Group metamorphic rock Weathering crust reservoir development model diagram **(a)** and the core photo of the weathering metamorphic strata in the Well XWD1, 997.83–998.26 m. **(b)** Plain scan photo. **(c)** Rolling scan photo.

petroleum system in the Awati Sag (Liang et al., 2004; Zhao et al., 2005; Zheng et al., 2008; Gao et al., 2010; Yang et al., 2010; Zhang et al., 2012a, 2022a, 2022c; Wang et al., 2013; Xi et al., 2016; Zhu et al., 2016, 2018, 2019). This study systematically reviews the parametric characteristics of two sets of marine and two sets of terrestrial source rocks to analyze the hydrocarbon generation potential, as summarized in Table 1.

Terrestrial hydrocarbon source rocks are primarily developed in the Mesozoic Jurassic and Triassic systems, mainly located in the northeastern region of the Wensu Salient. In these systems, the Jurassic Qiakemake Formation (J_2q) source rocks are mainly distributed in the Baicheng Sag, adjacent to the northern piedmont zone (Fig. 9(a)). The lithology predominantly consists of the shallow to semi-deep lacustrine mudstone, shale, and carbonaceous mudstone. These rocks possess an average total organic carbon (TOC) content of 2.03%, a vitrinite reflectance (R_o) ranging from 0.7% to 2.0%, and a thickness varying from 22 to 754 m, respectively. The kerogen type is mainly categorized as Type I–II_1 (Liang et al., 2004; Zhao et al., 2005; Zheng et al., 2008; Yang et al., 2010; Wang et al., 2013; Zhang et al., 2022a, 2022c).

The Triassic Huangshanjie Formation (T_3h) source rocks are situated closer to the Wensu Salient, with their sedimentary center shifted westward compared to the Jurassic source rocks. The thickness of the T_3h source rocks diminishes both to the north and south from the Baicheng area, exhibiting a distinctive thickness pattern of increasing toward the north and thinning toward the south, respectively (Fig. 9(b)). The lithology primarily comprises the shallow to semi-deep lacustrine mudstone, shale, and carbonaceous mudstone. They exhibit an average TOC of 1.03%, a vitrinite reflectance (R_o) spanning from 1.3% to 2.1%, a thickness ranging from 38 to 764 m, and the Type III kerogen, respectively (Liang et al., 2004; Zhao et al., 2005; Zheng et al., 2008; Yang et al., 2010; Wang et al., 2013; Zhang et al., 2022a, 2022c).

Marine hydrocarbon source rocks are primarily developed in the Lower Cambrian and Middle-Upper Ordovician systems, mainly distributed in the Awati Sag. In particular, the Ordovician Saergan Formation ($O_{2\text{-}3}s$) source rocks are predominantly composed of black shale interbedded with thin layers of limestone and limestone lenses in basin-to-slope facies (Fig. 9 (c)). The average TOC of the black mudstone is 2.88%, with a vitrinite reflectance (R_o) ranging from 2.03% to 2.85%, and a thickness varying from 4 to 28 m, predominantly featuring Type I–II_1 kerogen (Gao et al., 2010; Zhang et al., 2012a, 2022b, 2022c; Xi et al., 2016; Li et al., 2022; Xu et al., 2024; Zhu et al., 2024).

The Lower Cambrian Yuertusi Formation ($\in_1y$) constitutes a suite of high-quality hydrocarbon source rocks that are extensively distributed across the Tarim Basin (Fig. 9(d)). The lithological composition of the Yuertusi Formation predominantly includes black shale, black mudstone, black carbonaceous mudstone, and black carbonaceous shale, which were deposited in shelf-to-slope environments. These source rocks are associated with phosphorus-rich sediments and are believed to be related to upwelling oceanic currents. They exhibit an average TOC content of 5.5%, vitrinite reflectance (R_o) values ranging from 2.11% to 2.9%, and thickness varying from 10 to 55 m, respectively. The kerogen type is characterized as Type I–II_1 (Gao et al., 2010; Zhang et al., 2012a, 2020, 2022b, 2022c; Xi et al., 2016; Zhu et al., 2016, 2018; Li et al., 2022; Xu et al., 2024).

4.4. Hydrocarbon characteristics and correlations

(1) *Oil comparison*

The crude oil extracted from the weathered metamorphic reservoir within Well XWD1 is classified as medium crude oil, with a density of 0.9095 g/cm^3, a viscosity of 45.93 mm^2/s at 50 °C, a wax content that constitutes 1.63% of the oil's composition, and a freezing point of −21 °C respectively (Table 2).

The crude oil's compositional family is predominantly constituted by saturated hydrocarbons with a proportion of 57.2%, followed by aromatic hydrocarbons at 21.8% and non-hydrocarbons at 15.8%, respectively. The asphaltene content is relatively low, amounting to 5.2%. The oil displays a low ratio of saturated to aromatic hydrocarbons (2.62) and a higher ratio of resin to asphaltene (3.03). The Pr/Ph value of the crude oil is 2.04, which is higher than the values commonly observed in marine-origin crude oils from the Tabei area (typically less than 1.35) yet lower than that of the terrestrial crude oil from Well WUC1 in the Wushi Sag (3.35). This Pr/Ph value suggests that the primary sedimentary environment for the source rocks was characterized by weak oxidation to weak reduction conditions, which overall shares similarities with the characteristics of Neogene terrestrial crude oil (Li et al., 2010a, 2010b, 2015; Zhang et al., 2012b, 2022a).

The C_{27}–C_{28}–C_{29} regular sterane distribution in the crude oil from the weathered metamorphic reservoir exhibits a V-shaped pattern, with a pronounced development of rearranged steranes. The relative abundance of pregnane and low molecular weight tricyclic terpanes is notably lower. A successive decrease in the relative abundance of C_{19}–C_{22} tricyclic terpanes, which deviates

Table 1
Basic information of the two kinds of source rocks on the periphery of the Wensu Salient (modified from Zhang et al., 2022a).

Sags	Strata	Genetic types	Lithology	TOC, %	T_{max}, °C	S_1+S_2, mg·g^{-1}	PI	HI, mg/g	"A", %	Kerogen type	R_o, %	Thickness, m
Awati Sag	Cambrian Yuertusi Formation ($\in_1y$)	Marine facies	Black shale	5.5	500	0.62	–	3.5	0.086	I–II_1	2.11–2.9	10–55
	Ordovician Saergan Formation ($O_{2\text{-}3}s$)		Black Carbonaceous shale	2.88	460	2.17	–	116	0.012	I–II_1	2.03–2.85	4–28
Baicheng Sag	Jurassic Qiakemake formation (J_2q)	Lacustrine facies	Dark grey mudstone, shale	2.03	463	1.82	0.1	82.67	0.12	I–II_1	0.7–2.0	22–754
	Triassic Huangshanjie formation (T_3h)		Dark mudstone, shale	1.03	510	0.58	–	29	0.149	III	1.3–2.1	38–764

Note: all listed data are the average of tested samples. TOC: total organic carbon; S_1+S_2: genetic potential; PI: production index; HI: hydrocarbon index; "A": chloroform bitumen "A".

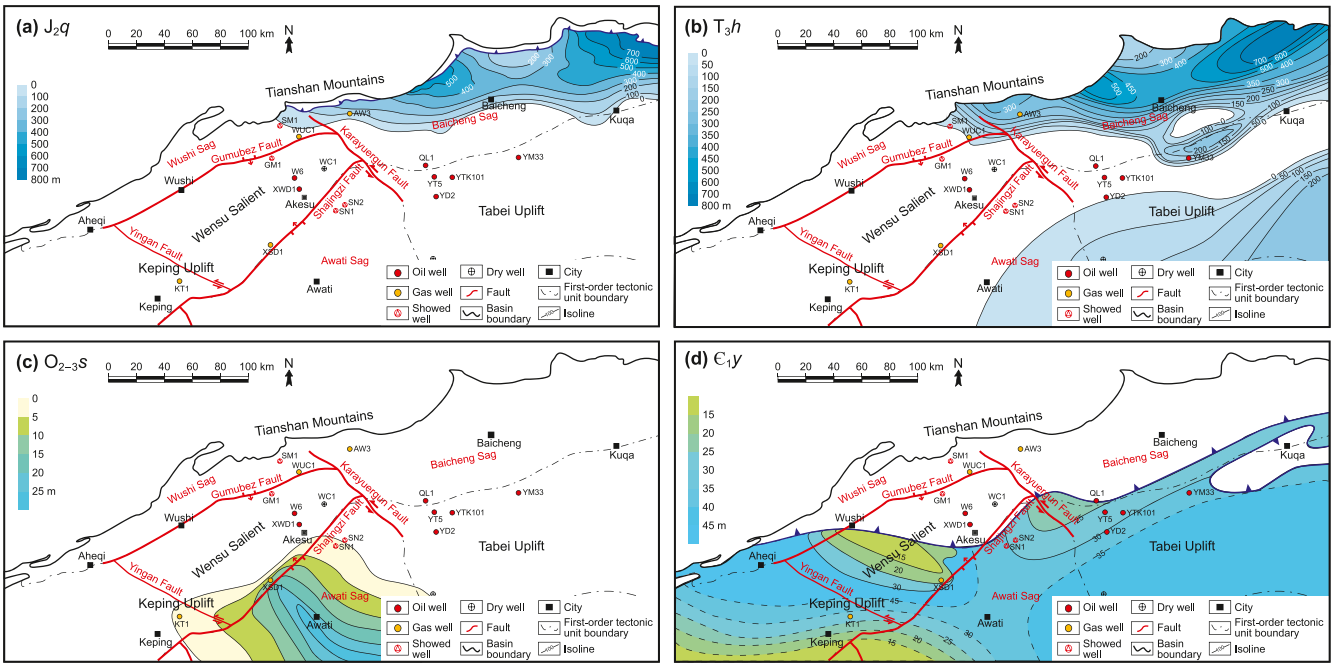

Fig. 9. Thickness map of four sets of source rocks around the Wensu Salient (modified after Zhang et al., 2022a).

Table 2
Physical properties and G.C. indices of partial oils analyzed (partial data are from Zhang et al., 2022a, 2022b).

Lab No.	Well	Strata	Depth, m	Density, g/cm^3*^{1}	Viscosity, mm^2/s*^{2}	Freeze point, °C	Wax, %	Sulfur, %	Sat, %	Aro, %	Resin, %	Asp, %	Pr/Ph
1	XWD-1	Pt_2ak	997.4–1017	0.9095	45.93	−21	1.63	–	57.2	21.8	15.8	5.2	2.04
2	XWD-1	N_1j	872.5–884.8	0.91	46.98	−30	4.48	–	58.3	20.9	15.8	5.1	1.68
3	SM1	K_1s	5138–5143	0.85	5.85	22	3.93	0.1	81.9	13.1	4.5	0.5	2.58
4	WUC1	K	6038.5–6053	0.86	2.86	10	21.1	0.19	85.1	12.6	2.2	0.2	3.35
5	YM33	∈	5503.5–5515.24	0.85	1.33	−45	11.2	0.19	27.12	49.44	9.89	27.12	2.01
6	YT5	K	5323–5325.5	0.80	3.30	21	15.99	–	87.55	7.11	3.75	1.58	2.31
7	YD2	K	4764–4767	0.81	1.53	13	12.67	–	–	–	–	–	2.48
8	YTK101	E	5329–5333	0.79	1.56	20	12.6	–	80.6	7.11	3.75	1.58	2.31
9	QL1	E-K	5775.2–5777	0.84	6.69	25	17.94	–	85.1	83	5.6	1.1	2.25
10	SN1	T	5095.5–5098.5	–	–	–	–	–	71.52	9.6	6.5	12.8	1.31
11	SN2	T	6110.5–6113.2	0.88	13.7	−6.0	3.30	0.25	71	8.8	5.8	14.2	1.27
12	XSD1	S	2380.35–2380.47	0.88	16.98	4	3.4	0	67.65	24.25	4.9	3.2	0.85

Note: *^{1}: 20 °C; *^{2}: 50 °C; Sat: saturated hydrocarbon; Aro: aromatic hydrocarbon; Asp: asphaltene; "-": undetected.

from the typical distribution observed in marine crude oils from the Awati Sag in Wells SN1, SN2, and XSD1 (Fig. 10). The presence of gammacerane is minimal, while the concentrations of C_{29} 25-norhopane and C_{30} diahopane are elevated (Fig. 10). These characteristics of the crude oil from the weathered metamorphic reservoir in the Wensu Salient are analogous to those found in continental crude oils in the Baicheng Sag from adjacent wells (SM1, WUC1, YM33, YT5, YD2, YTK101, QL1) (Fig. 10). The C_{29} sterane ααα20S/(S + R) and C_{29} sterane αββ/(ααα+αββ) values for the crude oil from the weathered metamorphic reservoir are 0.45 and 0.42, respectively, indicating crude oil is in mature stage.

(2) *Gas comparison*

Hu et al. (1993) established a genetic classification chart based on the relationship between $\delta^{13}C_2$ and $\delta^{13}C_1$ of natural gas, which is used to distinguish various types of parental material. Generally, a boundary of $\delta^{13}C_2 \approx -28$ ‰ is used to differentiate between humic and sapropelic natural gas (Dai, 1993). Natural gas with $\delta^{13}C_2 > -28$‰ is classified as humic, while gas with $\delta^{13}C_2 < -28$‰ is classified as sapropelic. The isotopic analysis in the Wensu Salient and its adjacent areas (Table 3 and Fig. 11(a)) indicates that the natural gas within the metamorphic rock reservoirs of the Pt_2ak formation in the Wensu Salient shares similarities with the natural gas from the N_1j formation. Specifically, they exhibit a dual genetic origin, with components attributed to both sapropelic and humic sources. The sapropelic component mainly derives from marine hydrocarbon source rocks located in the southeastern Awati Sag, while the humic component primarily originates from terrestrial hydrocarbon source rocks situated in the northeastern Baicheng Sag. Meanwhile, the natural gas from the Cambrian strata in wells XT1 and KT1, located at the southern margin of the Wensu Salient, primarily originates from marine hydrocarbon source rocks (Wang, 2024). The TT1 well, situated at the northeastern margin and closer to the Baicheng Sag, is of terrestrial sapropelic origin (Wang et al., 2023).

Xie et al. (2016) established a discriminant chart of $\ln(C_1/C_2)$ versus $\ln(C_2/C_3)$ for the identification of crude oil cracking gas and kerogen degradation gas through the high-temperature and high-pressure gold tube system and autoclave thermal simulation

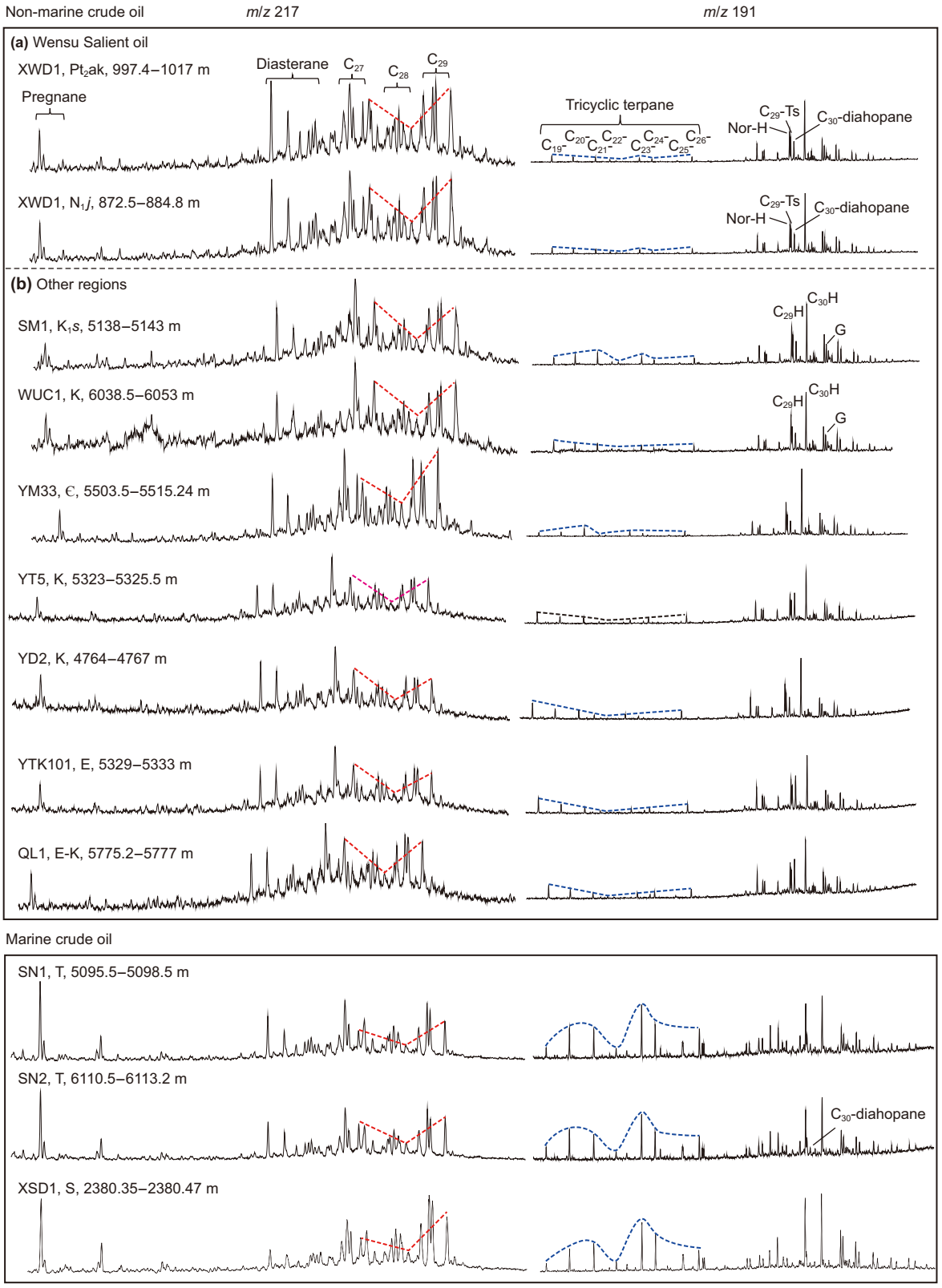

Fig. 10. $m/z = 217$ and $m/z = 191$ mass fragmentograms of saturated hydrocarbon fractions of the selected Lacustrine and marine oils (partial data are from Zhang et al., 2022c).

experiments on kerogen and crude oil. In particular, the $\ln(C_1/C_2)$ and $\ln(C_2/C_3)$ values of both types of natural gas increase with the degree of evolution; however, due to differences in the structure of crude oil and kerogen, the evolutionary trends of the two types of natural gas differ (the area below the red trend line in Fig. 11(b) represents crude oil cracking gas). The natural gas in the Wensu Salient and its periphery consists of both kerogen cracking gas and crude oil cracking gas (Table 4 and Fig. 11(b)). The natural gas in the metamorphic rock reservoirs of the Aksu Group is predominantly kerogen cracking gas, with a minor amount of crude oil cracking

Table 3
The carbon isotope characteristics of natural gas in the Wensu Salient and its periphery, and the corresponding maternal material types of source rocks.

Lab No.	Well	Depth, m	Strata	$\delta^{13}C_1$, ‰	$\delta^{13}Cco_2$, ‰	$\delta^{13}C_2$, ‰	$\delta^{13}C_3$, ‰	$\delta^{13}C_2-\delta^{13}C_1$, ‰	Gas source
1	W6	1606–1612	Pt_2ak	−48.3	–	−31.4	–	16.9	Early to mid-stage saprolite gas
2	W6	1618–1621	Pt_2ak	−43.2	–	−26.1	–	17.1	Early to mid-stage humic gas
3	W6-1	1566–1574	Pt_2ak	−35.4	–	−33.6	–	1.8	Late stage saprolite gas
4	W6-1	1578–1582	Pt_2ak	−42.9	–	−26.3	–	16.6	Early to mid-stage humic gas
5	KN1	5240–5245	Є	−37.6	−0.3	−34.7	−28.1	2.9	Late stage saprolite gas
6	XT1	6593.5–6800	Є	−47.7	–	−31.3	–	16.4	Early to mid-stage saprolite gas
7	TT1	5677.5–5690.5	Є	−39.4	−4.8	−26.5	−24.1	12.9	Early to mid-stage humic gas
8	W6	1192–1492.5	N_1j	−42.7	–	−25.8	–	16.9	Early to mid-stage humic gas
9	W7	1293.5–1303.5	N_1j	−46.6	–	−30.5	–	16.1	Early to mid-stage saprolite gas
10	W7-1	1400.5–1378	N_1j	−40.9	–	−26.7	–	14.2	Early to mid-stage humic gas
11	K2	2551–2559	N_1j	−45.7	–	−25.4	−23.1	20.3	Early to mid-stage humic gas
12	H79-10	2465–2470	N_1j	−39.3	–	−26.6	−24.6	12.7	Early to mid-stage humic gas

Note: drilling in the Pt_2ak and N_1j is situated within the main body of the Wensu Salient, whereas Cambrian drilling is located at its periphery (Fig. 1(b)).

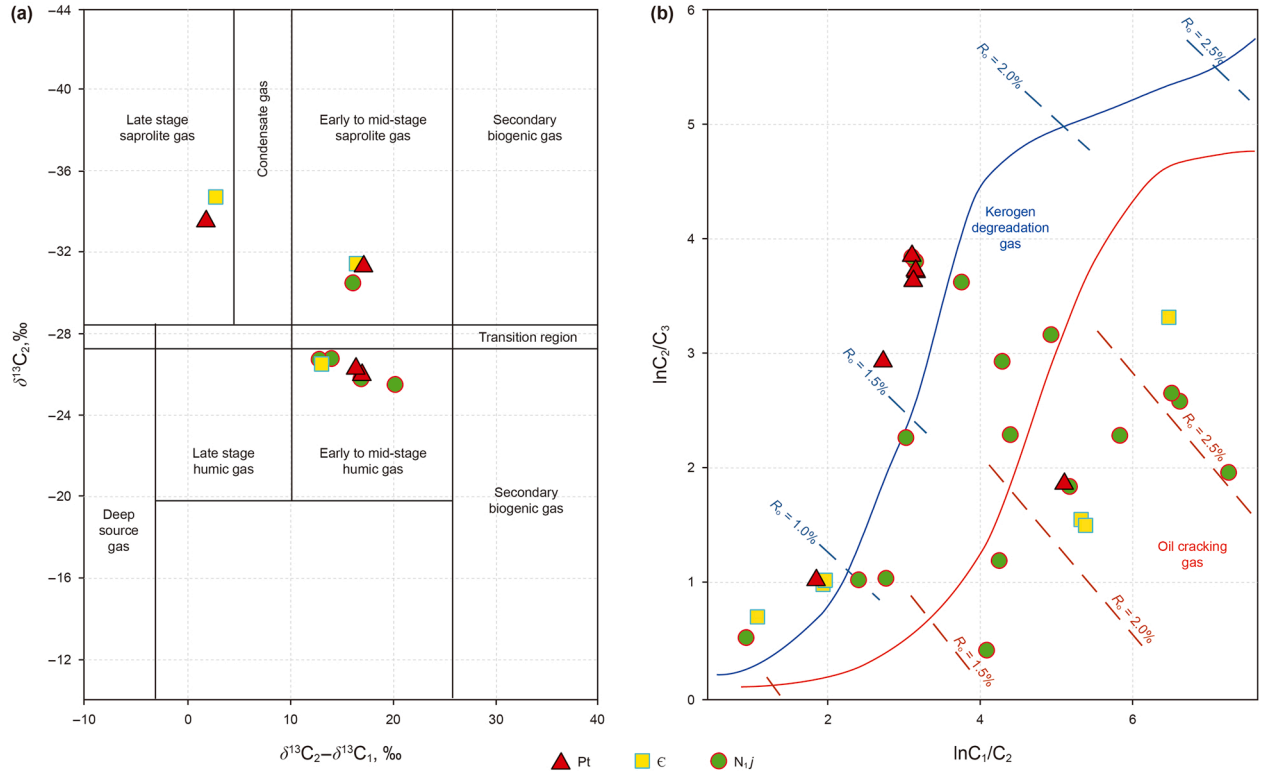

Fig. 11. (a) Natural gas parental material types identification in the Wensu Salient and its periphery (Hu et al., 1993; Dai, 1993). **(b)** The natural gas maturity and genetic identification chart (Xie et al., 2016).

gas. Furthermore, only the Paleozoic hydrocarbon source rocks in the Awati Sag had the conditions for cracking during the geological history (Cheng et al., 2022; Wang, 2024). Thus, the crude oil cracking gas originates from the marine hydrocarbon source rocks in the Awati Sag. Based on the comprehensive analysis of the test as mentioned above results, the collected gas can be featured as a mixed origin, which might derive from overmature marine source rocks in the Awati Sag, the marine oil cracking, and terrestrial source rocks in the northeastern Baicheng Sag, respectively.

5. Discussion

5.1. Hydrocarbon sources and accumulation stages

The two primary sets of marine source rocks in the Awati Sag have undergone a complex and prolonged hydrocarbon generation and expulsion history. The Cambrian Yuertusi Formation ($\in_1y$) source rock commenced hydrocarbon generation in the Ordovician, reached its peak oil generation during the Late Caledonian–Early Hercynian, and attained its peak gas generation in the Middle–Late Indosinian. At present, it is in a highly to over-mature stage (Fig. 12). The Ordovician Sargan Formation ($O_{2\text{-}3}s$) source rock began generating hydrocarbons in the Early Hercynian, entered its initial peak oil generation phase during the Late Hercynian–Early Indosinian, and is now in a mature to over-mature stage (Fig. 12) (Zhang et al., 2022a).

In the southeastern margin of the Wensu Salient, the XSD1 and SN1 wells have encountered hydrocarbons derived from marine source rocks in the Awati Sag within the Silurian and Permian formations, respectively (Zhang et al., 2022b, 2022d). Fluid inclusion analysis has confirmed three key hydrocarbon accumulation phases: the Late Caledonian–Early Hercynian, the Late Hercynian,

Table 4
Natural gas components in typical wells of the Wensu Salient and its periphery.

Lab No.	Well	Depth, m	Strata	CH_4, %	C_2H_6, %	C_3H_8, %	iC_4H_{10}, %	lnC_1/C_2, %	lnC_2/C_3, %
1	W6	1606–1612	Pt_2ak	88.97	9.9	0.22	0.07	2.20	3.81
2	W6	1618–1621	Pt_2ak	74.573	11.694	4.195	0.53	1.85	1.03
3	W6	1631–1648	Pt_2ak	94.07	3.94	0.1	0.05	3.17	3.67
4	W6	1650–1658	Pt_2ak	93.92	3.98	0.1	0.06	3.16	3.68
5	W6-1	1565–1574	Pt_2ak	98.72	0.594	0.092	0.1	5.11	1.87
6	W6-1	1578–1582	Pt_2ak	93.46	4.1	0.11	0.02	3.13	3.62
7	W6-1	1587–1591	Pt_2ak	91.79	5.89	0.32	0.17	2.75	2.91
8	W6-1	1591–1593	Pt_2ak	93.46	4.1	0.11	0.02	3.13	3.62
9	KN1	5240–5245	ϵ	59.29	0.28	0.06	0.03	5.36	1.54
10	KN1	5240–5246	ϵ	58.52	0.27	0.06	0.03	5.38	1.50
11	KT1	3686–3698	ϵ	90.228	0.137	0.005	0	6.49	3.31
12	TT1	5677.5–5690.5	ϵ	56.43	19.14	9.57	1.86	1.08	0.69
13	XT1	6593.5–6800	ϵ	74.875	10.46	3.964	0.556	1.97	0.97
14	XT1	6593.5–6800	ϵ	75.974	10.7	3.995	0.545	1.96	0.99
15	H6	1678.0–1692.0	N_1j	89.37	31.13	0.04	0	1.05	6.66
16	H11	2125–2139	N_1j	85.8	7.67	2.78	0.52	2.41	1.01
17	SK2	674.5–740	N_1j	98.72	0.29	0.03	0.04	5.83	2.27
18	SK2	842.0–852.5	N_1j	98.88	0.07	0.01	0.01	7.25	1.95
19	SK6	718.3–900.1	N_1j	98.93	0.56	0.09	0.09	5.17	1.83
20	W6	1490–1492.5	N_1j	93.91	3.98	0.09	0.05	3.16	3.79
21	W6	1192.0–1492.5	N_1j	97.04	0.13	0.01	0	6.62	2.56
22	W6-1	1602.2–1631.8	N_1j	93.89	3.97	0.09	0.05	3.16	3.79
23	W6-1	1315.5–1330	N_1j	95.26	2.21	0.06	0.02	3.76	3.61
24	W7	1293.5–1303.5	N_1j	76.25	1.28	0.86	0.36	4.09	0.40
25	W7-1	1400.5–1378	N_1j	94.53	1.29	0.07	0.04	4.29	2.91
26	W16	1708.5–1730.5	N_1j	93.28	4.13	0.09	0.05	3.12	3.83
27	W17	1818–1824	N_1j	89.96	5.62	2.01	0.44	2.77	1.03
28	W17	1574–1824	N_1j	96.79	0.7	0.03	0.01	4.93	3.15
29	W17	1270.5–1278	N_1j	94.43	0.14	0.01	0	6.51	2.64
30	W17	1554.5–1824	N_1j	95.7	1.17	0.12	0.05	4.40	2.28
31	W18	1502–1716	N_1j	96.94	1.37	0.42	0.11	4.26	1.18
32	W18	1714–1716	N_1j	57.04	22.03	13.26	2.85	0.95	0.51
33	W20	1625–1632.5	N_1j	93.18	4.47	0.47	0.18	3.04	2.25

Note: drilling in the Pt_2ak and N_1j is situated within the main body of the Wensu Salient, whereas Cambrian drilling is located at its periphery (Fig. 1(b)). The components such as N_2, CO_2, nC_4H_{10}, iC_5H_{12}, nC_4H_{10}, among other gases, are not listed in the table.

and the Himalayan (Zhang et al., 2022b). The Himalayan phase is primarily characterized by gas accumulations, sourced from both highly mature gas generated by the mature to over-mature marine source rocks and cracking gas derived from paleo-oil reservoirs formed in the Caledonian–Early Hercynian and Late Hercynian periods.

The northwestern Tarim Basin exhibits complex tectonic activity, with well-developed deep and large faults facilitating hydrothermal fluid migration from deep strata. Additionally, the extensive Large Igneous Province (LIP) in the Permian induced significant thermal anomalies, providing favorable temperature conditions for the cracking of paleo-oil reservoirs (Cheng et al., 2022; Wang, 2024). In the KN1 well, highly to over-mature solid bitumen has been discovered in the Cambrian sub-salt reservoir, which shows clear evidence of hydrothermal dissolution and alteration (Liu et al., 2023).

In contrast, the two sets of lacustrine source rocks in the northeastern Baicheng Sag underwent hydrocarbon generation and expulsion more recently. The Triassic Huangshanjie Formation (T_3h) source rocks reached peak oil generation between 23 Ma and 12 Ma, while the Jurassic Qiakemake Formation (J_2q) source rocks experienced hydrocarbon generation and expulsion between 5 Ma and 2 Ma (Fig. 12) (Wang et al., 2005; Li et al., 2007, 2010a, 2010b; Zhang et al., 2022b). The Neogene traps in the Wensu Salient were finalized at a later stage, and analyses such as fluid inclusion thermobarometry and hydrocarbon generation-expulsion history confirm that the crude oil in this area primarily originated from the source rocks in the northeastern Baicheng Sag. The main periods of hydrocarbon accumulation occurred at 17 Ma and 5 Ma (Li et al., 2010a, 2010b; Zhang et al., 2019, 2022a, 2022b, 2022c).

Based on the preceding analysis, the Wensu Salient has undergone continuous uplift from the Early Paleozoic to the Neogene. The metamorphic rock reservoirs within the Aksu Group in the central region did not finalize their trap structures until the Neogene. The timing of trap formation postdates the oil generation period of the marine source rocks in the southern region but aligns well with the oil generation timing of the continental source rocks in the northeastern region. Furthermore, the mass fragmentograms at $m/z = 217$ and $m/z = 191$ for crude oil in the metamorphic reservoirs of the Aksu Group within the Wensu Uplift show similarities to those of continental crude oils from the Baicheng Sag in the northeastern region (Fig. 10). Therefore, crude oil in the metamorphic rock reservoirs of the Wensu Salient is likely sourced from the T_3h and J_2q source rock formations, with the primary hydrocarbon accumulation periods occurring at approximately 17 Ma and 5 Ma.

The natural gas in the metamorphic rock reservoirs of the Aksu Group is predominantly kerogen cracking gas, with a minor amount of crude oil cracking gas. Furthermore, only the Paleozoic hydrocarbon source rocks in the Awati Sag had the conditions for cracking during the geological history (Cheng et al., 2022; Wang, 2024). Thus, the crude oil cracking gas originates from the marine hydrocarbon source rocks in the Awati Sag. Based on the comprehensive analysis of the test as mentioned above results, the collected gas can be featured as a mixed origin, which might derive from overmature marine source rocks in the Awati Sag, the marine

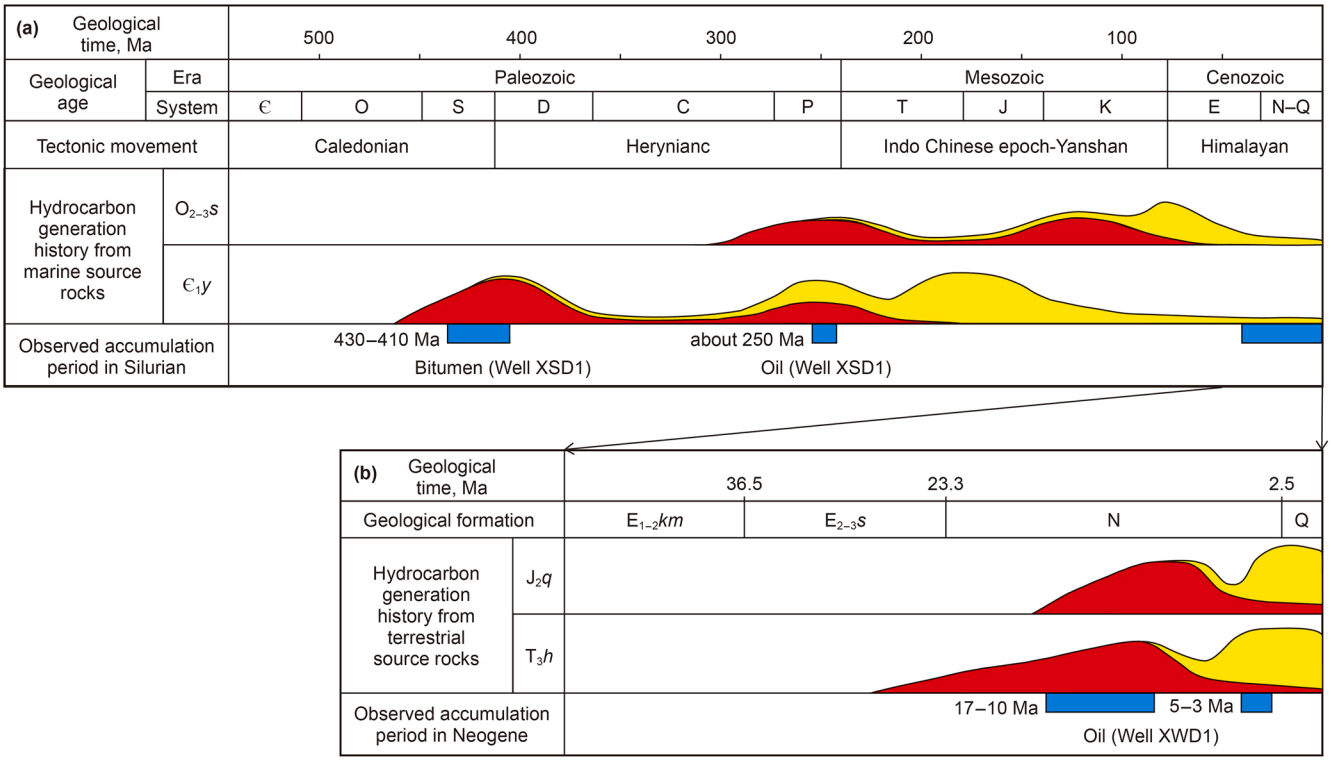

Fig. 12. The hydrocarbons generation history for two kinds of source rocks in the adjacent sags (modified from Li et al., 2015; Zhu et al., 2019; Zhang et al., 2022a, 2022b, 2022c). **(a)** Marine source rocks in the Awati sag. **(b)** Terrestrial source rocks in the Baicheng Sag.

oil cracking, and terrestrial source rocks in the northeastern Baicheng Sag, respectively. The timing of gas charge has persisted from the trap formation period to the present.

5.2. Hydrocarbon migration pathways

The Gumubez Fault Zone in the northern Wensu Salient (Fig. 1(b)) extends approximately 180 km and consists of the deep-seated South Wushi Fault and the shallow Gumubiezi Fault, which exhibit different dip directions. The former originated during the terminal Caledonian to Early Hercynian orogeny and was subsequently reactivated in the Late Hercynian to Indosinian period, undergoing northward subduction. The latter, in contrast, is a shallow reverse fault that formed in the Late Cenozoic due to the influence of the Himalayan orogeny (He et al., 2011; Liu et al., 2022). The Shajingzi Fault along the southeastern margin extends about 163 km and comprises an early deep-seated wedge-shaped thrust structure and a later basement-involved thrust structure. The early thrust system formed during the Caledonian collisional orogeny, whereas the latter emerged during the Late Permian to Early Triassic and continued its activity intermittently until it became fully developed in the mid-Neogene (Qi et al., 2014; Zhang et al., 2022b). To the east, the Karayuergun Fault Zone extends approximately 70 km and similarly consists of two distinct fault systems at different depths. The deep-seated fault was formed during the Late Permian to Cretaceous, whereas the shallow fault underwent folding and thrusting primarily in the Miocene, evolving into a strike-slip fault system during the Pleistocene (Zhang et al., 2019; Liu et al., 2022).

Evidently, the faults surrounding the Wensu Salient are characterized by their large scale and prolonged activity, directly connecting to the hydrocarbon source rocks in the surrounding hydrocarbon-generating depressions. These faults serve as the primary vertical migration pathways for hydrocarbons (Fig. 13).

The complex tectonic evolution of the Wensu region has not only given rise to an intricate fault system but has also resulted in the formation of a major unconformity at the top of the Aksu Group metamorphic rocks. Due to the significant velocity and density contrast between this unconformity and the overlying sedimentary layers, it exhibits prominent strong reflection characteristics on seismic profiles (Fig. 13). North of the field extinction line (Fig. 1(b)), this unconformity extends over an area of approximately 3000 km^2, serving as a primary lateral migration pathway for hydrocarbons. Additionally, numerous secondary faults with a northeast-southwest orientation have developed along this unconformity. These faults predominantly manifest as linear, northeast-southwest-oriented thrust faults with relatively small displacement and scale, although some can extend regionally up to 20 km (as shown in Fig. 14). Clearly, these structures further enhance the efficiency of lateral hydrocarbon migration from the Baicheng Sag in the northeastern Wensu Salient to the Awati Sag in the southeast.

Moreover, we observed that seismic events beneath the uppermost layer of the tight metamorphic strata (denoted by green arrowheads in Fig. 13) might indicate ancient buried hills or paleo-anticlines. These reflections are characterized by significant clarity and are readily distinguishable from coherent multiples. In the absence of drilling through these strata to date, we hypothesize that the internal metamorphic layers exhibiting lamellar reflections may constitute prospective oil and gas-bearing reservoirs, akin to the productive inner buried hills within the Archean metamorphic basement of the Bohai Bay Basin (Meng et al., 2009; Yu et al., 2019; Xue et al., 2021).

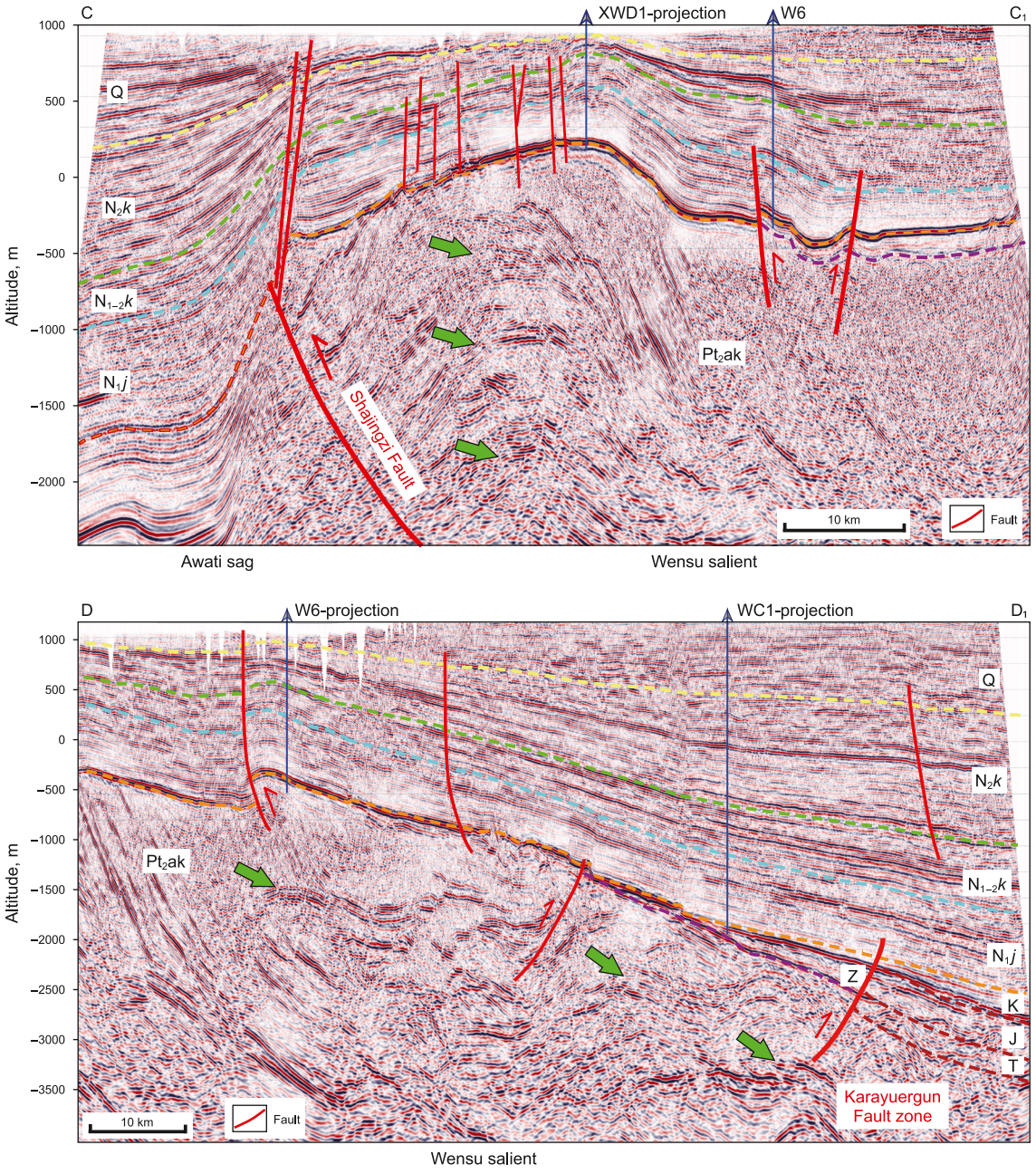

Fig. 13. Typical seismic sections in the research area (section locations are CC_1 and DD_1 in Fig. 15).

5.3. Oil-gas accumulation model

In summary, an oil and gas accumulation model characterized by "multi-source hydrocarbon supply and late-stage reservoir formation" can be established for the Aksu Group metamorphic rock reservoirs in the Wensu Salient (Fig. 14). Although the Wensu Salient itself lacks hydrocarbon source rocks, the large-scale terrestrial hydrocarbon source rocks to the northeast and the marine hydrocarbon source rocks to the southeast possess the significant hydrocarbon generation and expulsion durations, which can provide ample oil and gas resources. The Aksu Group strata experienced a prolonged uplift before being covered by the Neogene strata, forming a regional unconformity. The metamorphic rock surface beneath the unconformity has undergone the long-term weathering and erosion, potentially creating favorable weathered crust reservoirs. Simultaneously, controlled by the dual compression of the northern Gumubez fault and the southern Shajingzi fault, the Wensu Salient's metamorphic rock layers have developed multiple northeast-trending secondary faults (Fig. 15), resulting in a complex fracture system. This system, along with the metamorphic rocks' low porosity and low permeability characteristics, forms a fractured metamorphic rock reservoir. Despite experiencing persistent uplift and erosion from the Late Caledonian until the onset of stable deposition in the Middle–Late Neogene, the metamorphic core of the Wensu Salient was subjected to extensive weathering and a prolonged period of reservoir potential development. The modification of reservoir quality, especially within fractured reservoirs, was critically controlled by the evolution of the two boundary faults: the Shajingzi Fault to the south and the Gumubiezi Fault to the north.

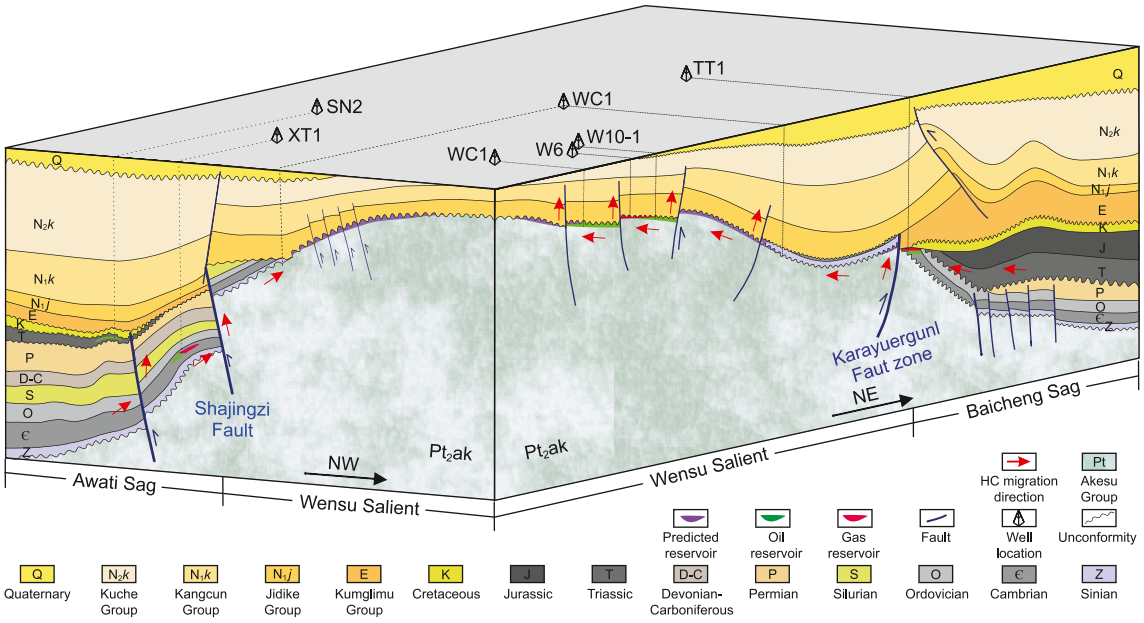

Fig. 14. Constructed oil-gas accumulation model of the weathering metamorphic reservoir in the Wensu Salient.

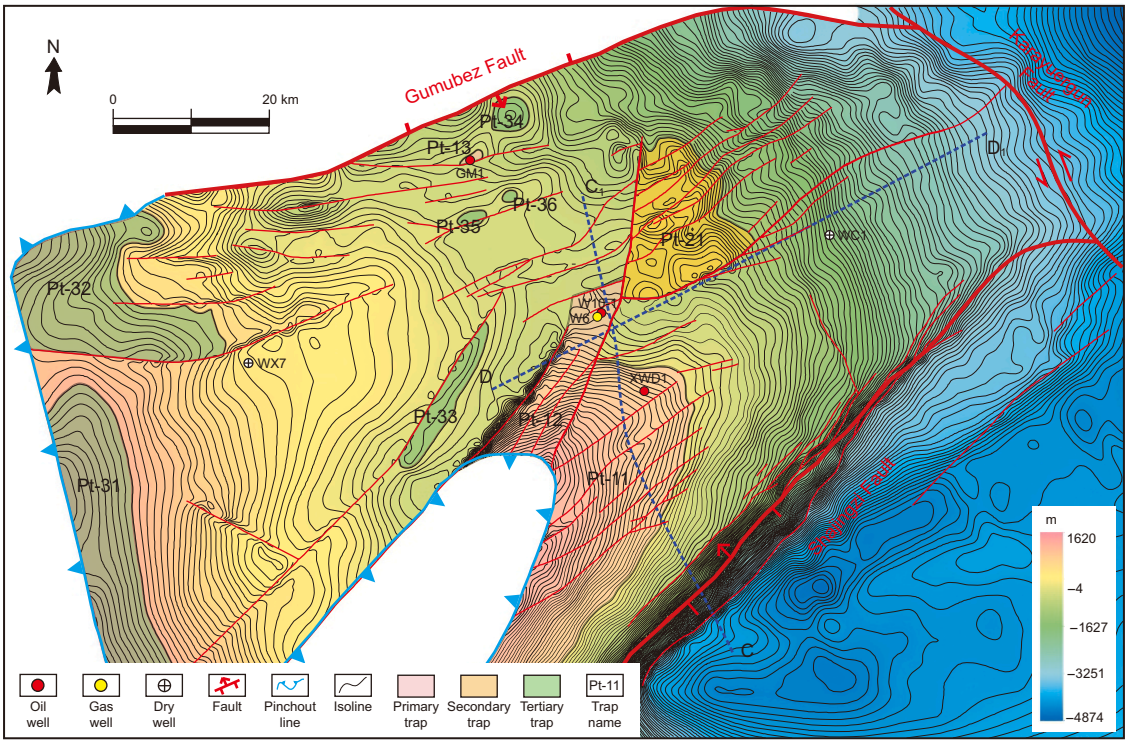

Fig. 15. Trap distribution map of the weathering metamorphic crust in the Wensu Salient.

These faults were particularly active during the Late Hercynian and Indosinian–Yanshanian orogenies (Jia, 2005; Cui and Tang, 2011; Wang et al., 2009; He et al., 2011; Qi et al., 2014; Liu et al., 2022; Zhang et al., 2022d). As a result, these two periods represent the most significant phases of modification for the metamorphic rocks, substantially enhancing the fracture density and thus the quality of the fractured reservoirs.

The Neogene Jidike Formation (N_1j) in the Wensu Salient exhibits an average thickness of 445.79 m, of which mudstone accounts for 341.9 m, yielding a mudstone-to-formation ratio of 76.7%. Individual mudstone beds vary from 1 m to 40 m in thickness, averaging 3–7 m. Petrophysical measurements on core samples from the well XWD1 demonstrate average values of 12.64% for porosity, 0.105 mD for permeability, and 0.95 MPa for

breakthrough pressure (Zhang et al., 2019). Collectively, these parameters confirm the suitability of the Jidike Formation as a competent regional seal for hydrocarbon entrapment. The traps in the metamorphic rock layers are primarily structural and structural-stratigraphic traps closely related to the fault system.

The Wensu Salient formed a large nose-shaped structural setting with a high western limb and a low eastern limb during the late stage of the Himalayan movement. The traps in the Aksu Group metamorphic rock layers were finalized at this time. Through fault systems such as the Gumubez, Shajingzi, and Karayuergun, as well as the unconformity surfaces, these traps are connected to the surrounding hydrocarbon-rich depressions, making them favorable for oil and gas migrations and accumulations. Specifically, the crude oil generated from the Jurassic and Triassic hydrocarbon source rocks in the Baicheng sag of the northeast entered the metamorphic rock reservoirs through the fault and unconformity surfaces during the periods of 17 Ma and 5 Ma, thus forming oil reservoirs. After the metamorphic rock traps were finalized, high-maturity gas generated from the Cambrian–Ordovician marine hydrocarbon source rocks in the Awati sag, the cracked gas from marine crude oil in the Awati sag, and the terrestrial source rock gas from the Baicheng sag could continuously enter the metamorphic rock reservoirs along complex paths involving faults and unconformity surfaces, leading to the hydrocarbon accumulation.

Within the same trap, hydrocarbons are accumulated at higher positions and underwent the physical differentiation (i.e., Well W6 reveals a gas reservoir, and Well W10-1 reveals an oil reservoir, as shown in Fig. 14). The structural position of Well WC1 on the northern slope of the Wensu Salient is generally lower, with the Sinian dolomite reservoir mainly producing water and a subtle amount of natural gas. Better oil and gas accumulation may be present at the up-dip higher positions. Overall, the Aksu Group metamorphic rock reservoirs in the Wensu Salient possess many hydrocarbon sources, and the hydrocarbon accumulation is generally late.

5.4. Petroleum exploration potential

Utilizing the geological-geophysical joint calibration and detailed structural modeling analysis on twenty-two collected 2D seismic lines, the tectonic horizon and fault system of the top metamorphic reservoirs within the Proterozoic Aksu Group are systematically interpreted for trap classification and evaluation following drilling data. The topographic map of the metamorphic bedrock depicts a nose-like paleo-uplift structure that is elevated in the southwest and dips towards the northeast (Fig. 15). It is essentially demarcated from adjacent hydrocarbon-generating sags by various fault systems. Overall, this structure extends in the northeast direction from the outcrop in the southwest to an area with a burial depth exceeding 6000 m in the northeast (Fig. 15).

Based on the available data, a total of ten structural (including fault nose, anticline, or faulted anticline) or stratigraphic traps have been meticulously identified within the weathering metamorphic bedrock of the Proterozoic Aksu Group, encompassing a total area of 860.5 km^2 (Table 5). These identified traps are closely associated with fault systems (Fig. 15), which not only facilitate weathering processes and efficient oil and gas migration pathways but also provide the necessary sealing conditions in conjunction with the overlying Neogene shales. Specifically, these traps have been further categorized into three grades based on their hydrocarbon-bearing potential, with the most promising traps confirmed by successful drillings accounting for a gross area of 386.7 km^2 (Table 4).

Table 5
Factor table for the weathering metamorphic traps in the Wensu Salient (Fig. 15).

Trap name	Trap type	Area, km^2	Amplitude, m	Shallowest burial depth, m	Shallowest altitude, m	Trap grade
Pt-11	Fault nose; Stratigraphic trap	305.5	1300	60	1150	I
Pt-12	Stratigraphic trap	75.9	1850	20	1250	I
Pt-13	Stratigraphic trap	5.3	100	1600	−450	I
Pt-21	Fault nose	111.8	600	1490	−400	II
Pt-31	Stratigraphic trap	169.6	500	20	1550	III
Pt-32	Fault nose; Stratigraphic trap	153.3	650	130	1100	III
Pt-33	Fault nose	26.2	150	1300	−150	III
Pt-34	Anticline	8.9	100	1600	−450	III
Pt-35	Faulted anticline	2.8	50	1490	−350	III
Pt-36	Anticline	1.2	50	1500	−350	III

Table 6
Predicted trap reserve for the most favorable weathering metamorphic traps in the Wensu Salient.

Trap name	Trap area, km^2	Average effective thickness, m	Average effective porosity, %	Average oil saturation, %	Oil density, g/cm^3	Oil volume factor (/)	Trap reserve (One hundred million ton)
Pt-11	305.5	14.3	3	35	0.9038	1	0.41
Pt-12	75.9	14	4	38	0.9019	1	0.15
Pt-13	5.3	20	3	40	0.9228	1	0.01

Excluding those traps that have not yet been proven by drilling, the reserves of the three traps classified as Level I are estimated in principle through the horizon comparison, structural analysis, and drilling data by employing the mathematical volume method (Zhang et al., 2022c):

$$N = 100AH\varphi(1 - S_{wi})\rho_o/B_{oi} \quad (1)$$

where N is the predicted geological trap reserve, A is the trap area, H is the average effective thickness, φ is the average effective porosity, S_{wi} is the original water saturation, ρ_o is the average oil density, and B_{oi} is the average oil volume factor, respectively.

In detail, the specific parameters for the most favorable traps, including Pt-11, Pt-12, and Pt-13, are derived from the drilling data of Wells XWD1, W10-1, and GM1, respectively (Table 6). The three Grade I traps are collectively estimated to obtain a total geological hydrocarbon resource of 5.7×10^7 tons in the Wensu Salient.

6. Conclusions

(1) Although the Aksu Group of the Proterozoic strata in the Wensu Salient is geologically ancient and its basement metamorphic rocks are generally dense, the prolonged history of uplift and reworking has facilitated the formation of weathering crust reservoirs at the top of the metamorphic rock section. The primary effective reservoir spaces consist of fractures and dissolution pores. The high-quality reservoir intervals exhibit an average porosity of approximately 4% and a permeability ranging from 0.061 mD to 1.5 mD. These reservoirs can form favorable stratigraphic and

structural traps in association with the Neogene Jidike Formation mudstone.

(2) The discovered crude oil in the metamorphic reservoir of the Aksu Group in the Wensu Salient is primarily sourced from the T_3h and J_2q formation source rocks in the northeastern Baicheng Sag, with major hydrocarbon accumulation periods at 17 Ma and 5 Ma. In contrast, the discovered natural gas originates from a mixture of cracked gas from marine crude oil, gas from lacustrine source rocks, and highly mature gas from marine source rocks, with gas charging continuing from the time of trap formation to the present.

(3) Although the Wensu Salient lacks source rock development, it is adjacent to the hydrocarbon-generating sags of Awati and Baicheng and features a fault-unconformity system that facilitates communication with source rocks. These geological conditions are favorable for hydrocarbon accumulation. Overall, the hydrocarbon accumulation in this region is characterized by a multi-source rock supply and late-stage reservoir formation.

(4) The most prospective metamorphic traps collectively cover an area of 386.7 km^2, yielding a preliminary resource estimate of up to 5.7×10^7 tons. Multileveled internal reservoirs may be present within the metamorphic strata of the Wensu Salient, as indicated by analogous seismic reflections. Therefore, identifying efficient hydrocarbon migration pathways and valid traps is critical for the success of any exploration efforts in the area.

CRediT authorship contribution statement

Yuan-Yin Zhang: Writing – review & editing, Writing – original draft, Visualization, Validation, Supervision, Software, Resources, Project administration, Methodology, Investigation, Funding acquisition, Formal analysis, Data curation, Conceptualization. **Ze-Zhang Song:** Writing – original draft, Validation, Software, Investigation, Formal analysis, Data curation, Conceptualization. **Zhong-Kai Bai:** Supervision, Resources, Project administration, Methodology, Investigation, Funding acquisition, Data curation, Conceptualization. **Xing-Zheng Liu:** Writing – review & editing, Validation, Supervision, Methodology, Data curation. **Zi-Yu Zhang:** Writing – review & editing, Validation, Resources, Project administration, Investigation, Data curation.

Data availability

Data will be made available on request.

Declaration of competing interest

The authors declare that they have no known competing financial interests or personal relationships that could have appeared to influence the work reported in this paper.

Acknowledgments

This work was jointly supported by the National Major Project of China (Grant No. 2025ZD1010303), the Special Project of the Department of Science and Technology of Inner Mongolia Autonomous Region (Grant No. KCX2024003), the projects of the China National Petroleum Corporation (Grant Nos. 2024DJ93 and ZY25-XN138-FW1011-02), and China Geological Survey Projects (Grant No. DD20241675). The authors extend their gratitude to Dr. Xue-Song Li at Zhongman Oil & Gas Company, Dr. Lin Wu at the Institute of Geomechanics, Chinese Academy of Geological Sciences, and Professors Sumei Li at China University of Petroleum-Beijing for their valuable suggestions.

References

Areshev, E.G., Dong, T.L., San, N.T., Shnip, O.A., 1992. Reservoirs in fractured basement on the continental shelf of southern Vietnam. J. Petrol. Geol. 15, 451–464. https://doi.org/10.1111/j.1747-5457.1992.tb01045.x.

Belaidi, A., Bonter, D.A., Slightam, C., Trice, R.C., 2018. The Lancaster field: progress in opening the UK's fractured basement play. Pet. Geol. Conf. Proc. 385–398. https://doi.org/10.1144/PGC8.20.

Bonter, D.A., Trice, R., 2019. An integrated approach for fractured basement characterization: the Lancaster field, a case study in the UK. Pet. Geosci. 25 (4), 400–414. https://doi.org/10.1144/petgeo2018-152.

Burwood, R., Redfern, J., Cope, M.J., 2003. Geochemical Evaluation of East Sirte Basin (Libya) Petroleum Systems and Oil Provenance, vol 207. Geological Society, London, Special Publications, pp. 203–240. https://doi.org/10.1144/GSL.SP.2003.207.1.

Chang, J., Qiu, N.S., Li, J.W., 2012. Tectono-thermal evolution of the northwestern edge of the Tarim Basin in China: Constraints from apatite (U-Th)/He thermochoronology. J. Asian Earth Sci. 61, 187–198. https://doi.org/10.1016/j.jseaes.2012.09.020.

Chen, W.Y., Zhu, G.Y., Zhang, K.J., Zhang, Y.J., Yan, H.H., Du D., D., Zhang, Z.Y., Xia, B., 2020. Late Neoproterozoic intracontinental rifting of the Tarim carton, NW China: An integrated geochemical, geochronological and Sr–Nd–Hf isotopic study of siliciclastic rocks and basalts from deep drilling cores. Gondwana Res. 80 (2020), 142–156. https://doi.org/10.1016/j.gr.2019.10.007.

Cheng, X.X., Wu, H.X., Sun, D.H., Huang, W.K., Chen, H.L., Lin, X.B., Zhu, K.Y., Zhang, F.Q., 2022. The Permian mafic intrusive events in the northwestern margin of the Tarim Basin and their tectonic significance. Acta Petrol. Sin. 38 (3), 743–764. https://doi.org/10.18654/1000-0569/2022.03.09 (in Chinese).

Cui, J.W., Tang, Z.M., 2011. Tectonic framework of the Tarim basinand its tectonic stress field analysis. Acta Petrol. Sin. 27 (1), 231–242.

Dai, J.X., 1993. The carbon-hydrogen isotopic characteristics of natural gas and the identification of various types of natural gas. Nat. Gas Geosci. 4 (2–3), 1–40. https://doi.org/10.11764/j.issn.1672-1926.1993.02.1 (in Chinese).

Ding, H., Ma, D., Lin, Q., Jing, L., 2015. Age and nature of Cryogenian diamictites at Aksu, Northwest China: implications for Sturtian tectonics and climate. Int. Geol. Rev. 57 (16), 2044–2064. https://doi.org/10.1080/00206814.2015.1050463.

Dong, X., Zhang, Z.M., Tang, W., 2011. Precambrian tectono-thermal events of the northern margin of the Tarim Craton: Constraints of zircon U-Pb chronology from high-grade metamorphic rocks of the Korla. Acta Petrol. Sin. 27, 47–58. https://doi.org/10.1002/cbdv.200690119 (in Chinese).

Dou, L., Cheng, D., Wang, J., Du, Y., Xiao, G., Wang, R., 2020. Petroleum systems of the Bongor Basin and the great Baobab oilfield, southern Chad. J. Petrol. Geol. 43, 301–321. https://doi.org/10.1111/jpg.12767.

Gao, X.Z., Pang, X.Q., Li, X.G., Chen, Z.Y., Shan, J.F., Liu, F., Zou, Z.W., Li, W.L., 2008. Complex petroleum accumulating process and accumulation series in the buried-hill trend in the rift basin: An example of Xinglongtai structure trend, Liaohe subbasin. Sci. China, Ser. A D 51 (2), 108–116. https://doi.org/10.1007/s11430-008-6022-9.

Gao, Z.Y., Zhang, S.C., Li, J.J., Zhang, B.M., Gu, Q.Y., Lu, Y.H., 2010. Distribution and sedimentary environments of Saergan and Yingshan shales of the Middle-Uppler Ordovician in western Tarim Basin. J. Palaeogeogr. 12 (5), 599–608. https://doi.org/10.7605/gdlxb.2010.05.009 (in Chinese).

Ge, R., Zhu, W., Wilde, S.A., He, J., Cui, X., Wang, X., Zheng, B.H., 2014. Neoproterozoic to paleozoic long-lived accretionary orogeny in the northern Tarim Craton. Tectonics 33 (3), 302–329. https://doi.org/10.1002/2013TC003501.

He, D.F., Sun, F.Y., He, J.Y., Wen, Z., Ge, J., Song, Z.Y., 2011. Geometry and kinematics of Wensubei-Yeyungou fault and its implication for the genetic mechanism of North Tarim uplift. Chin. Geol. 38 (4), 917–933. https://doi.org/10.3969/j.issn.1000-3657.2011.04.010 (in Chinese).

He, J., Zhu, W., Ge, R., Zheng, B., Wu, H., 2014. Detrital zircon U-Pb ages and Hf isotopes of Neoproterozoic strata in the Aksu area, northwestern Tarim Craton: Implications for supercontinent reconstruction and crustal evolution. Precambr. Res. 254, 194–209. https://doi.org/10.1016/j.precamres.2014.08.016.

Hu, T.L., Ge, B.X., Chang, Y.G., Liu, B., 1993. The development and application of fingerprint parameters for hydrocarbons absorbed by source rocks and light hydrocarbons in natural gas. Nat. Gas Geosci. 12 (4), 375–394. https://doi.org/10.11781/sysydz199004375 (in Chinese).

Jia, C.Z., 1997. Structural Characteristics of Tarim Basin, China. Petroleum Industry Press, Beijing, Beijing (in Chinese).

Jia, C.Z., 2005. Foreland thrust-fold belt features and gas accumulation in Midwest China. Petrol. Explor. Dev. 32 (4), 9–15. https://doi.org/10.3321/j.issn:1000-0747.2005.04.002 (in Chinese).

Jia, C.Z., Wei, G.Q., Yao, H.J., 1995. Oil and Gas Exploration Books in Tarim Basin-tectonic Evolution and Regional Structural Geology. Petroleum Industry Press, Beijing, Beijing (in Chinese).

Jiang, Z.X., Li, Z., Li, F., Pang, X.Q., Yang, W., Liu, L., Jiang, F., 2015. Tight sandstone gas accumulation mechanism and development models. Pet. Sci. 12 (4), 587–605. https://doi.org/10.1007/s12182-015-0061-6.

Jin, Q., Zhao, X.Z., Jin, F.M., Ma, P., Wang, Q., Wang, J., 2014. Generation and accumulation of hydrocarbons in a deep "buried hill" structure in the Baxian depression, Bohai Bay Basin, Eastern China. J. Petrol. Geol. 37 (4), 391–404. https://doi.org/10.1111/jpg.12592.

Koning, T., 2003. Oil and Gas Production from Basement Reservoirs: Examples from Indonesia, USA and Venezuela, vol 214. Geological Society, London, Special Publications, pp. 83–92. https://doi.org/10.1144/GSL.SP.2003.214.01.05.

Krishna, K.S., 2003. Structure and evolution of the Afanasy Nikitin seamount, buried hills and 85 °E Ridge in the northeastern Indian Ocean. Earth Planet Sci. Lett. 209 (3–4), 379–394. https://doi.org/10.1016/S0012-821X(03)00081-5.

Li, F., Liu, X.X., Chen, J.F., Wang, R., Wang, Y.Y., Chen, Z.Z., 2022. Palaeo-environmental evolution and organic matter enrichment of Eopalaeozoic shales, northwestern Tarim Basin, China: Integrated organic and inorganic geochemistry approach. Palaeogeogr. Palaeogl. 601, 111123. https://doi.org/10.1016/j.palaeo.2022.111123.

Li, S.M., Amrani, A., Pang, X., Yang, H., Said-Ahmad, W., Zhang, B., Pang, Q., 2015. Origin and quantitative source assessment of deep oils in the Tazhong Uplift, Tarim Basin. Org. Geochem. 78 (6), 1–22. https://doi.org/10.1016/j.orggeochem.2014.10.004.

Li, S.M., Pang, X.Q., Jin, Z.J., Yang, H.J., Xiao, Z.Y., Gu, Q.Y., Zhang, B.S., 2010a. Petroleum source in the Tazhong Uplift, Tarim Basin: New insights from geochemical and fluid inclusion data. Org. Geochem. 41 (6), 531–553. https://doi.org/10.1016/j.orggeochem.2010.02.018.

Li, S.M., Pang, X.Q., Zhang, B.S., Xiao, Z.Y., Gu, Q.Y., 2010b. Oil-source rock correlation and quantitative assessment of mixed Ordovician oils in Tazhong Uplift, Tarim Basin. Pet. Sci. 7, 179–191. https://doi.org/10.1007/s12182-010-0025-9.

Li, Q., Wang, F.Y., Kong, F.Z., Xiao, Z.R., Chen, K.Y., 2007. Characteristics of J2q source rocks in Kuqa Depression. J. Oil Gas Technol. 29 (6), 38–42. https://doi.org/10.3969/j.issn.1000-9752.2007.06.009 (in Chinese).

Liang, D.G., Chen, J.P., Zhang, B., Zhang, S.C., Wang, F.Y., Zhao, M.J., 2004. Nonmarine Hydrocarbons Generation from Kuqu Depression, Tarim Basin. Petroleum Industry Press, Beijing. Beijing (in Chinese).

Liu, C.W., Hu, Y.Z., Ren, T., He, A.B., Dong, C.Q., Zhang, Y.H., Ma, L., 2017. Study on the petrographic features and protoliths reconstruction of Akesu Group metamorphic rocks from the northwestern margin of Tarim Basin, the Xingjiang Uygur Autonomous region, China. Acta Mineral. Sin. 37 (5), 617–624. https://doi.org/10.16461/j.cnki.1000-4734.2017.05.012 (in Chinese).

Liu, G.P., Zeng, L.B., Li, H.N., Ostadhassan, M., Rabiei, M., 2020. Natural fractures in metamorphic basement reservoirs in the Liaohe Basin. China. Mar. Petrol. Geol. 119, 104479. https://doi.org/10.1016/j.marpetgeo.2020.104479.

Liu, L.H., Han, M., Gao, Y.J., Zhang, Y.Y., Liu, C.X., Duan, Y., Yang, Y.X., Jiang, K.P., 2023. Main reservoir controlling factors and diagenetic evolution of the Xiaoerbulak Formation of Tarim Basin, NW China: Case study of Well Kepingnan 1 in Keping area. Nat. Gas Geosci. 34 (5), 763–779. https://doi.org/10.11764/j.issn.1672-1926.2023.01.013 (in Chinese).

Liu, X.J., Hou, M.C., Niu, C.M., Wang, Q.B., Zhang, X.T., Ye, T., Cui, P.Y., Hao, Y.W., 2021. Mesozoic-Cenozoic tectonic controls on the formation of large-scale metamorphic rock buried-hill reservoirs in Bozhong Sag, eastern China. Geol. J. 56 (10), 5109–5124. https://doi.org/10.1002/gj.4226.

Liu, Y.L., Gao, Y.J., Zhang, J.F., Bai, Z.K., Cheng, M.H., Zhang, Y.Y., Yang, Y.X., 2022. New understanding of tectonic characteristic of the Wensu salient in Tarim Basin. Acta Petrol. Sin. 38 (9), 2665–2680. https://doi.org/10.18654/1000-0569/2022.09.09 (in Chinese).

Long, X., Yuan, C., Sun, M., Zhao, G., Xiao, W., Wang, Y., Yang, Y., Hu, A., 2010. Archean crustal evolution of the northern Tarim Craton, NW China: Zircon U-Pb and Hf isotopic constraints. Precambr. Res. 180 (3–4), 272–284. https://doi.org/10.1016/j.precamres.2010.05.001.

Lyu, Q.X., Wang, W.M., Jiang, Q.C., Yang, H.F., Deng, H., Zhu, J., Liu, Q.G., Li, T.T., 2023. Basement reservoirs in China: Distribution and factors controlling hydrocarbon accumulation. Minerals 13 (8), 1052. https://doi.org/10.3390/min13081052.

Ma, L., Liu, Q.X., Zhang, J.L., Wei, P.S., Chen, Q.L., Zhang, H.Q., 2006. A discussion of exploration potentials of basement hydrocarbon reservoir. Nat. Gas. Ind. 26, 8–11. https://doi.org/10.3321/j.issn:1000-0976.2006.01.003 (in Chinese).

Meng, W.G., Chen, Z.Y., Li, P., Guo, Y.M., Gao, X.Z., Hui, X.F., Zhang, Y.L., 2009. Exploration theories and practices of buried-hill reservoirs: A case from Liaohe Depressions. Petrol. Explor. Dev. 36 (2), 136–143. https://doi.org/10.1016/S1876-3804(09)60116-6.

Paridiguli, B., Xie, H.W., Cheng, X.G., Wu, C., Zhang, Y.Q., Xu, Z.P., Lin, X.B., Chen, H.L., 2020. Deformation features and tectonic transfer of the Gumubiezi Fault in the northwestern margin of Tarim Basin, NW China. Petrol. Explor. Dev. 47 (4), 753–761. https://doi.org/10.1016/S1876-3804(20)60090-8.

Parnell, J., Baba, M., Bowden, S., Muirhead, D., 2017. Subsurface biodegradation of crude oil in a fractured basement reservoir, Shropshire, UK. J. Geol. Soc. 174, 655–666. https://doi.org/10.1144/jgs2016-129.

Qi, Q.J., Zhang, Z.C., Dong, S.Y., Zhang, D.Y., Huang, H., Zhang, S., Ma, T.L., 2011. Geochemical characteristics and tectonic setting of Mesoproterozoic metamorphic rocks in Aksu area, Southwestern Tianshan Mountains. Acta Petrol. Et Mineral. 30 (2), 172–184. https://doi.org/10.3969/j.issn.1000-6524.2011.02.002 (in Chinese).

Qi, Y.M., Li, Y.J., Wang, Y.R., Liu, Y.L., Zhu, H.Y., Liu, L.W., Mo, T., Chen, Y.G., 2014. Fault analysis on Shajingzi structural belt, NW margin of Tarim Basin, NW China. Chin. J. Geol. 47 (2), 265–277. https://doi.org/10.3969/j.issn.0563-5020.2012.02.001 (in Chinese).

Riber, L., Dypvik, H., Sørlie, R., 2015. Altered basement rocks on the Utsira high and its surroundings, Norwegian North Sea. Nor. J. Geol. 95 (1), 57–89.

Schubert, F., Diamond, L.W., Tóth, T.M., 2007. Fluid-inclusion evidence of petroleum migration through a buried metamorphic dome in the Pannonian Basin, Hungary. Chem. Geol. 244 (3), 357–381. https://doi.org/10.1016/j.chemgeo.2007.05.019.

Tian, N.X., Chen, W.X., Huo, H., Tian, J.B., Wu, J., 2008. Petroleum geological characteristics and favorable hydrocarbon accumulation zone prediction in the Silt Basin, Libya. Oil Gas Geol. 29, 485–490. https://doi.org/10.3321/j.issn:0253-9985.2008.04.011 (in Chinese).

Tong, K.J., Zhao, C.M., Lv, Z.B., Zhang, Y.C., Zheng, H., Xu, S.N., Wang, J.L., Pan, L.L., 2012. Reservoir evaluation and fracture characterization of the metamorphic buried hill reservoir in Bohai Bay. Petrol. Explor. Dev. 39, 56–63. https://doi.org/10.1016/S1876-3804(12)60015-9 (in Chinese).

Trice, R., Hiorth, C., Holdsworth, R., 2022. Fractured basement play development on the UK and Norwegian rifted margins. Geol. Soc. London, Spec. Publ. 495, 73–97. https://doi.org/10.1144/SP495-2018-174.

Wang, F.Y., Du, Z.L., Li, Q., Zhang, S.C., Chen, J.P., Xiao, Z.R., Liang, D.G., 2005. Organic maturity and hydrocarbon generation history of the Mesozoic oil-prone source rocks in Kuqa Depression, Tarim Basin. Geochimica 34 (2), 136–145. https://doi.org/10.3321/j.issn:0379-1726.2005.02.006 (in Chinese).

Wang, G.L., Li, Y.J., Sun, J.H., Huang, Z.B., Zhao, Y., Liu, Y.L., 2009. Structural deformation characteristics of the Kalpin thrust belt, NW Tarim. Chin. J. Geol. 44 (1), 50–62. https://doi.org/10.3321/j.issn:0563-5020.2009.01.005 (in Chinese).

Wang, J., Zhao, L., Zhang, X., Yang, Z., Cao, H., Chen, L., Shan, F., Liu, M., 2015. Buried hill karst reservoirs and their controls on productivity. Petrol. Explor. Dev. 42 (6), 852–860. https://doi.org/10.1016/S1876-3804(15)30082-3.

Wang, Q., Laubach, S.E., Gale, J., Ramos, M.J., 2019. Quantified fracture (joint) clustering in archean basement, Wyoming: Application of normalized correlation count method. Pet. Geosci. 25 (4), 415–428. https://doi.org/10.1144/petgeo2018-146.

Wang, Q.H., 2024. Breakthrough and significance of oil and gas exploration of Upper Cambrian Xiaqiulitage Formation in Kalayuergun structural belt, western Tabei uplift. Acta Petrol. Sin. 45 (5), 615–627. https://doi.org/10.7623/syxb202404001 (in Chinese).

Wang, Q.H., Yang, H.J., Cai, Z.Z., Yang, X.Z., Zhang, L., Jiang, J., Zhou, L., 2023. Major breakthrough and significance of petroleum exploration in Well Tuotan 1 on the south slope of Kuqa Depression, Tarim Basin. China Petrol. Explor. 28 (5), 28–42. https://doi.org/10.3969/j.issn.1672-7703.2023.05.003 (in Chinese).

Wang, Z.M., Xie, H.W., Li, Y., Lei, G.L., Wu, C., Yang, X.Z., Ma, Y.J., Neng, Y., 2013. Exploration and discovery of large and deep subsalt gas fields in Kuqa foreland thrust belt. China Petrol. Explor. 18 (3), 1–11. https://doi.org/10.3969/j.issn.1672-7703.2013.03.001 (in Chinese).

Wu, L., Feng, X.Q., Guan, S.W., Zhu, G.Y., Yang, H.J., 2022. Proterozoic basin-orogen framework in the northern Tarim Craton, China. Precambr. Res. 373, 106627. https://doi.org/10.1016/j.precamres.2022.106627.

Wu, L., Guan, S.W., Ren, R., Zhang, C.Y., Feng, X.Q., 2021. Neoproterozoic glaciations and rift evolution in the northwest Tarim Craton, China: New constraints from geochronological, geochemical, and geophysical data. Int. Geol. Rev. 63 (1), 1–20. https://doi.org/10.1080/00206814.2019.1700399.

Wu, L., Guan, S.W., Zhang, S.C., Yang, H.J., Jin, J.Q., Zhang, X.D., Zhang, C.Y., 2018. Neoproterozoic stratigraphic framework of the Tarim Craton in NW China: Implications for rift evolution. J. Asian Earth Sci. 158, 240–252. https://doi.org/10.1016/j.jseaes.2018.03.003.

Xi, Q., Yu, H.Z., Gu, Q.Y., Qian, L., Li, X.S., Li, M.F., 2016. Main hydrocarbon source rocks and contrasts for Awati Sag in Tarim Basin. Pet. Geol. Oilfield Dev. Daqing 35 (1), 12–18. https://doi.org/10.3969/J.ISSN.1000-3754.2016.01.003 (in Chinese).

Xie, Z.Y., Li, Z.S., Wei, G.Q., Li, J., Wang, D.L., Wang, Z.H., Dong, C.Y., 2016. Experimental research on the potential of sapropelic kerogen cracking gas and discrimination of oil cracking gas. Nat. Gas Geosci. 27 (6), 1057–1066. https://doi.org/10.11764/j.issn.1672-1926.2016.06.1057 (in Chinese).

Xu, C.G., Wang, Q.B., Zhu, H.T., Liu, X.J., Feng, C., Hu, B., Li, H., Hao, Y.W., Jin, X.Y., Jia, Y., 2024. Hydrothermal alteration mechanisms of an Archaean metamorphic buried hill and the models for reservoir zonation, Bozhong depression, Bohai Bay Basin. China. Mar. Petrol. Geol. 164, 106843. https://doi.org/10.1016/j.marpetgeo.2024.106843.

Xu, S.J., Wang, J., Wu, N., Xu, Q.H., 2024. Geochemical characteristics of Cambrian bitumen and Cambrian-Ordovician source rocks in the Keping area, NW Tarim Basin. Front. Earth Sci. 11, 1323705. https://doi.org/10.3389/feart.2023.1323705.

Xue, Y., Zhao, M., Liu, X.J., 2021. Reservoir characteristics and controlling factors of the metamorphic buried hill of Bozhong Sag, Bohai Bay Basin. J. Earth Sci. China. 32 (4), 919–926. https://10.1007/s12583-021-1415-1.

Yang, M.H., Jin, Z.J., Lv, X.X., Sun, D.S., Zeng, P., 2010. Tectono-sedimentary evolution of piggy-back basin: Example from Kuqa fold and thrust Belt, Northern Tarim Basin, northwest China. J. Earth Sci. 21 (4), 412–442. https://doi.org/10.1007/s12583-010-0104-2.

Ye, T., Chen, A., Niu, C., Wang, Q., Hou, M., 2022. Characteristics, controlling factors and petroleum geologic significance of fractures in the Archean crystalline basement rocks: A case study of the South Jinzhou oilfield in Liaodong Bay depression, North China. J. Petrol. Sci. Eng. 208, 109504. https://doi.org/10.1016/j.petrol.2021.109504.

Yu, Z.H., Du, Y.B., Xiao, K.Y., Wang, J.C., Xiao, G.J., Zhang, G.L., Liang, Q.F., 2019. Characteristics and influence factors of basement buried-hill reservoir in

Bongor Basin. Chad. Acta Petrol. Sin. 35 (44), 1279–1290. https://doi.org/10.18654/1000-0569/2019.04.20 (in Chinese).
Zhang, C.L., Li, Z.X., Li, X.H., Ye, H.M., 2009. Neoproterozoic mafic dyke swarms at the northern margin of the Tarim Block, NW China: Age, geochemistry, petrogenesis and tectonic implications. J. Asian Earth Sci. 35 (2), 167–179. https://doi.org/10.1016/j.jseaes.2009.02.003.
Zhang, C.Y., Guan, S.W., Wu, L., Ren, R., Wang, L.N., Wu, X.Q., 2020. Depositional environments of early Cambrian marine shale, northwestern Tarim Basin, China: Implications for organic matter accumulation. J. Petrol. Sci. Eng. 194, 107497. https://doi.org/10.1016/j.petrol.2020.107497.
Zhang, H.F., Wang, X., Zhang, K., Shi, C.Q., Fan, S., Lou, H., Wang, X.X., Li, G., 2022a. Oil-source correlation and accumulation evolution in Wushi-Wensu area of Tarim Basin. Nat. Gas Geosci. 33 (1), 24–35. https://doi.org/10.11764/j.issn.1672-1926.2021.07.007 (in Chinese).
Zhang, J., Yu, S., Gong, J., Li, H., Hou, K., 2013. The latest Neoarchean- Paleoproterozoic evolution of the Dunhuang block, eastern Tarim craton, northwestern China: Evidence from zircon U-Pb dating and Hf isotopic analyses. Precambr. Res. 226, 21–42. https://doi.org/10.1016/j.precamres.2012.11.014.
Zhang, J., Zhang, C.L., Li, H.K., Ye, X.T., Geng, J.Z., Zhou, H.Y., 2014. Revisit to time and tectonic environment of the Aksu blueschist terrane in northern Tarim, NW China: New evidence from zircon U-Pb age and Hf isotope. Acta Petrol. Sin. 30 (11), 3357–3365 (in Chinese).
Zhang, J.F., Gao, Y.J., Yang, Y.X., Zhou, X.G., Zhang, J.H., Zhang, Y.Y., 2019. Oil exploration breakthrough in the Wensu salient, northwest Tarim Basin and its implications. Petrol. Explor. Dev. 46 (1), 14–24. https://doi.org/10.11698/PED.2019.01.02.
Zhang, J.F., Zhang, Y.Y., Gao, Y.J., 2022b. Silurian hydrocarbon exploration breakthrough in the Shajingzi structural belt of northwest Tarim Basin and its implications. Petrol. Explor. Dev. 49 (1), 233–246. https://doi.org/10.1016/S1876-3804(22)60019-3.
Zhang, J.H., Yang, Y.X., Gao, Y.J., Li, S.M., Yu, B.S., Gong, X.X., Bai, Z.K., Miao, M.Q., Zhang, Y.Y., Sun, Z.C., Qi, Z.L., 2022c. Geochemistry and source of crude oils in the Wensu uplift, Tarim Basin, NW China. J. Petrol. Sci. Eng. 208, 109448. https://doi.org/10.1016/j.petrol.2021.109448.
Zhang, S.C., Gao, Z.Y., Li, J.J., Zhang, B.M., Gu, Q.Y., Lu, Y.H., 2012a. Identification and distribution of marine hydrocarbon source rocks in the Ordovician and Cambrian of the Tarim Basin. Petrol. Explor. Dev. 39 (3), 285–293 (in Chinese).
Zhang, S.C., Zhang, B., Yang, H.J., Zhu, G.Y., Su, J., Wang, X., 2012b. Adjustment and alteration of hydrocarbon reservoirs during the late Himalayan period, Tarim Basin, NW China. Petrol. Explor. Dev. 39 (6), 668–679. https://doi.org/10.1016/S1876-3804(12)60096-2.
Zhang, X.N., Yao, Y.B., Zhang, G.B., Ma, R.Y., Wang, Z.F., 2023. Natural fractures in a metamorphic buried hill reservoir, Bozhong 19–6 area, Bohai Bay Basin. China. Mar. Petrol. Geol. 155, 106402. https://doi.org/10.1016/j.marpetgeo.2023.106402.
Zhang, Y.Y., Zhang, J.F., Gao, Y.J., 2022d. Characteristics and accumulation model of Silurian tight sandstone gas reservoir: A case study in the Shajingzi belt, northwest Tarim Basin, China. Front. Earth Sci. 10, 437–448. https://doi.org/10.3389/feart.2022.857053.
Zhao, W.Z., Zhang, S.C., Wang, F.Y., Bernhard, C., Chen, J.P., Sun, Y.G., Zhang, B.M., Zhao, M.J., 2005. Gas systems in the Kuche Depression of the Tarim Basin: Source rock distributions, generation kinetics and gas accumulation history. Org. Geochem. 36, 1583–1601. https://doi.org/10.1016/j.orggeochem.2005.08.016.
Zheng, M., Peng, G.X., Lei, G.L., Guo, H.Q., Huang, S.Y., Wu, C., Li, Y.J., 2008. Structural pattern and its control on hydrocarbon accumulations in Wushi sag, Kuche depression, Tarim Basin. Petrol. Explor. Dev. 35 (4), 444–451. https://doi.org/10.1016/s1876-3804(08)60092-0.
Zhu, B., Guo, T.T., Liu, C.H., Pan, W.Q., Chen, Y.Q., Zhang, Y.G., Yang, T., 2024. Coastal upwelling and redox variations in the northwestern Tarim Basin (northwest China) during the middle-late Ordovician: Implication for paleo-depositional conditions of the organic matter enrichment in the Saergan Formation. Front. Earth Sci. 11, 1321488. https://doi.org/10.3389/feart.2023.1321488.
Zhu, G.Y., Chen, F.R., Chen, Z.Y., Zhang, Y., Xing, X., Tao, X.W., Ma, D.B., 2016. Discovery and basic characteristics of the high-quality source rocks of the Cambrian Yuertusi Formation in Tarim Basin. Nat. Gas Geosci. 27 (1), 8–21 (in Chinese).
Zhu, G.Y., Chen, F.R., Wang, M., Zhang, Z.Y., Ren, R., Wu, L., 2018. Discovery of the lower Cambrian high-quality source rocks and deep oil and gas exploration potential in the Tarim Basin, China. AAPG Bull. 102 (10), 2123–2151. https://doi.org/10.1306/03141817183.
Zhu, G.Y., Zhang, Z.Y., Zhou, X.X., Li, T.T., Han, J.F., Sun, C.H., 2019. The complexity, secondary geochemical process, genetic mechanism and distribution prediction of deep marine oil and gas in the Tarim Basin, China. Earth Sci. Rev. 198 (6), 1–28. https://doi.org/10.1016/j.earscirev.2019.102930.
Zhu, W.B., Zheng, B.H., Shu, L.S., Ma, D.S., Wu, H.L., Li, Y.X., Huang, W.T., Yu, J.J., 2011. Neoproterozoic tectonic evolution of the Precambrian Aksu blueschist terrane, northwestern Tarim, China: Insights from LA-ICP-MS zircon U-Pb ages and geochemical data. Precambr. Res. 185 (3–4), 215–230. https://doi.org/10.1016/j.precamres.2011.01.012.